Theses and Dissertations

2016

Estimating Local Average Power In A Line-Of-Sight Indoor Channel: Spatial Sampling And Processing

Israt Jahan Disha
University of South Carolina

Follow this and additional works at: http://scholarcommons.sc.edu/etd

Part of the Electrical and Electronics Commons

ESTIMATING LOCAL AVERAGE POWER IN A LINE-OF-SIGHT INDOOR CHANNEL:
SPATIAL SAMPLING AND PROCESSING

By

Israt Jahan Disha

Bachelor of Science
University of Dhaka, 2010

_____

Submitted in Partial Fulfillment of the Requirements

For the Degree of Master of Science in

Electrical Engineering

College of Engineering and Computing

University of South Carolina

2016

Accepted by:

David W. Matolak, Director of Thesis

Guoan Wang, Reader

Lacy Ford, Senior Vice Provost and Dean of Graduate Studies

DEDICATION

To my parents

ABSTRACT

Modeling of indoor radio channels has been a dynamic area of research in recent years because of the increasing demand for indoor wireless communications. In order to efficiently deploy such indoor systems, a good knowledge of the indoor wireless channel's characteristics are required. One important characteristic is an accurate propagation path loss model. For developing such models various measurements have been carried out. In modeling propagation path loss in complex indoor environments, accurate and fast algorithms for estimating the local mean signal level are essential; these are also of use for power control and handoff decisions. These local mean power levels are typically characterized statistically. This thesis seeks to add to the body of knowledge regarding indoor channels by determining important parameters for estimating local mean power in line-of-sight (LOS) conditions.

In this thesis, a set of indoor channel measurements was taken, and from these measurements, statistical channel characteristics were derived. These characteristics, or parameters, include the spatial averaging window length ($2L$), interval between spatial samples (d_{min}), and the number of sampling points (N_{min}) within the window. These parameters are used in estimating the local mean value of a radio signal. Measurements were conducted in a LOS condition in a corridor at a frequency of 5.725 GHz, at nine different link distances (from 4.57 m to 41.15 m). A window based weighed sample average power estimator was used to determine the statistical characteristics of local

average power at each link distance. Computer simulations were also performed in order to verify the algorithm's performance before application to the measured data set. A set of relationships among *2L*, d_{min} and N_{min} were also established. It was observed that as the link distance increases in our LOS corridor environment, the number of sampling points, N_{min} and averaging window length *2L* tend to decrease. The decrease with link distance is not perfectly monotonic due to inhomogeneities in the environment, yet the general trend is as expected due to the wave guiding effect of the corridor. Future work in this area would include additional measurements in different corridors, and in different LOS indoor settings, with the aim of determining general guidelines for the estimation parameter values in such environments.

TABLE OF CONTENTS

LIST OF TABLES

ix

LIST OF FIGURES

CHAPTER 1

INTRODUCTION

1.1   Brief History of Wireless Communication

Wireless communication is considered to be one of the most revolutionary engineering breakthroughs in the course of human civilization. The rapid technological advancement of wireless communication has facilitated a variety of applications and standards. For examples, mobile communication, wireless sensor networks, satellite, radar and navigation, local area networks, body area networks, etc., are often viewed as blessings to mankind in the modern era. However, if we look back to some of the earliest communication systems such as the transmission and interpretation of sounds by different species or the use of lighthouses to navigate ships in the ocean, these systems also did not require any wires or cables for an effective communication. The oldest "electromagnetic" (optical) communications such as smoke signals are based on propagation of optical signals along a line-of-sight (LOS) path. Some other simple examples of wireless communications are flashing mirrors, signal flares, or semaphore flags [1].

The basis of electromagnetic wave propagation laid by Maxwell and Hertz instigated the access of modern wireless communication theory and practices. Just after their groundbreaking work, Tesla demonstrated the transmission of information via electromagnetic waves for the very first time, even though Marconi's demonstration of wireless communications from a boat to the Isle of Wight in the English Channel in the year 1898 was well-publicized [1].

The invention of telegraph and telephone systems in 1838 and 1895, respectively, has laid the foundation of radio communication for its development and considerable expansion [2]. In 1915, the first wireless voice transmission was established [2]. However, the first radio mobile telephone invented in 1924 was a major development in mobile radio communication systems. During the two world wars, research and developments on radio increased by a large extent. In the 1950's and 60's, there were numerous advancements in the wireless field, out of which the main concept developed for commercial systems was the cellular concept. The first and foremost, significant, scientific (and manufacturing) work intended at providing wireless communication broadly to the entire world was the development of the cellular concept by Bell Laboratories in the 1960's and 1970's [3]. By using this cellular concept, a larger number of users could operate on the same frequencies without significantly disturbing one another. This was possible via the frequency re-use concept, which enabled a given portion of frequency spectrum to be reused after a sufficient separation distance. The first cellular concept design was tested and deployed in Chicago in 1983, and this opened the field for new opportunities to use wireless technologies [2].

In the early 1980's, when users were inexperienced at using mobile radio telephones, the 1st generation (1G) cellular was developed based on analog technology, primarily to carry narrow band circuit-switched voice services using frequency modulation (FM) and frequency division multiple access (FDMA) techniques [2]. The first commercial "1st generation" (1G) cellular telephone system in the US, the Advanced Mobile Phone Services (AMPS) system, was deployed in 1983. Popular systems using 1G were the Nippon Telephone and Telegraph (NTT) system, Nordic Mobile Telephone

(NMT), Total Access Cellular System (TACS), Radiocom 2000, Japanese Total Access Cellular System (JTACS), and the Narrowband Total Access Cellular System (NTACS) [4].

After 1G voice communication systems, the second generation (2G) mobile systems evolved from the 1G system in the early 1990's. These could provide email, voice mail, and paging services using digital modulation schemes, and both time division multiple access (TDMA) and code division multiple access (CDMA). The Global System for Mobile Communications (GSM), the Interim Standard 136 (IS-136) (also known as US Digital Cellular), Pacific Digital Cellular (PDC), and cdmaOne (IS-95) are some of the popular 2G standards [3].

In order to meet the larger required data rates and improve spectral efficiency, newer sets of cellular systems appeared as 3G systems [3]. The 3G systems enabled the single mobile customer to use not only voice calls but also conduct internet browsing and reception of streaming audio and video. The 3G systems were designed to accommodate a number of services: ubiquitous connectivity, worldwide roaming, increased data rates (up to 2 Mbps), and enhanced capacity. In a nutshell, the third generation (3G) mobile systems were the first broadband multimedia mobile telecommunications technologies. Coverage is provided by a combination of cell sizes ranging from indoor pico-cells to global satellite cells. CdmaOne, also known as Cdma 2000, was developed on the basis of the IS 95 and IS 95B standards. The wideband CDMA (W-CDMA) system was developed based on the GSM principles and is also called Universal Mobile Telecommunication Service (UMTS). CdmaOne provides high data rates and high quality of service compared to the older 2G and 2.5G standards.

While 3G networks are still on board, the next generation fourth generation (4G) communication system have been developed. Along with 3G systems, 4G systems (sometimes also called 3.9G) have developed with the capability of providing even more advanced mobile wireless communication. They are offering 100 times faster data transfer than the 3G systems [2]. For 4G networks, Multiple Input Multiple Output system-Orthogonal Frequency Division Multiplexing (MIMO-OFDM) is the modulation and multiplexing method of choice. Nowadays, access to TV programming (either live TV or prerecorded programs) from cell phones is one of the most popular, innovative features using 4G standards. In addition, most road and rail network manufacturers are concentrating on the use of 4G Long-Term Evolution (LTE) technology. Some other features of 4G systems include IP packet-switched networks, mobile ultra-broadband (gigabit speed) access and multi-carrier transmission. International Mobile Telecommunications Advanced (IMT-Advanced), and Wi-MAX are also using 4G technologies.

1.2   Why Wireless Channel Modeling is Required

Even though modern 4G systems are able to provide higher data rates, there is still much focus needed to enhance the performance of indoor and outdoor radio coverage since the success of these systems still depends on how efficiently the mobile radio channel is utilized in these environments. For modeling such a channel, one of the most important factors is the attenuation of electromagnetic waves through the channel. A wireless signal confronts several channel features such as path loss (a synonym of attenuation), delay and phase shift, noise, and possibly shadowing, and interference, etc. [5]. Modeling of indoor/outdoor wireless channels helps in determining how the channel

4

affects the transmitted signal quantitatively in terms of estimating received signal power variation; wideband models also quantify any channel-induced distortion [6-9]. It is thus important to model channels in order to avoid difficulties in the design and implementation of networks and also to obtain a minimum system design cost without compromising the quality of service. Therefore, characterization and modeling of a channel is an essential step to analyze, evaluate and design a communication system.

1.3   Overview of Indoor Channel Modeling

Characterization of indoor radio propagation channels began to receive a lot of attention with the advent of the 3G wide area wireless networks. The indoor radio channel differs from the traditional radio channel in two aspects: a smaller coverage distance and a relatively greater environmental variability. Thus, modeling an indoor mobile radio channel is challenging because of significant variation of the channel within a small distance. The indoor radio channel is affected by several factors including building structure, layout of rooms, and the type of construction materials used. From a communication link perspective , there are three major channel characteristics that are important in modeling an indoor wireless channel: path loss, small-scale fading (multipath), and shadowing (local mean power variation) [2]. Path loss is simply the ratio of the transmit power to the receive power, or in other words, the attenuation of the channel. Small scale fading occurs when there is fluctuation of the received signal over short distances (fraction of wavelength) due to the reception of multiple replicas of the transmitted signal that have traveled different paths. Shadowing (variation of the local mean power) is generally a more slowly varying large-scale fading, and occurs due to objects obstructing the propagation path between the transmitter and the receiver.

Therefore, estimation of the local mean power of a radio signal is of importance in mobile communication systems in order to properly design the systems. Such estimation enables the construction of path loss models that provide designers with expected channel attenuations, thus constraining link distances and transmitter and receiver parameters. Knowledge of path loss can improve the system performance and help provide requirements for channel access, handoff, power control, etc. The efficiency of the use of the wireless channel is hence in some sense dictated by the accuracy of local mean signal power estimation.

1.4   Motivation

The aim of this work is to estimate the local average power (over a "small" area) for the purposes of determining effective and efficient methods of obtaining accurate local power estimates, specifically in line-of-sight (LOS) indoor settings. Experiments were conducted at a frequency of 5.725 GHz. The ultimate goal is to provide quantitative methods and guidelines that will help researchers develop accurate path loss models for line of sight (LOS) environments. For estimating local average power, it is necessary to determine three main parameters which are as follows:

➢ the minimum number of wavelengths (2L) over which to evaluate (this is the "extent" of the local area);

➢   the minimum value of the total number of points (N) within the 2L distance to average out small scale fading;

➢ the minimum separation (d) between the N samples to ensure that they are uncorrelated.

1.5   Thesis Outline

This thesis is divided into five chapters.

Chapter 1 provides an overview of the growth of the wireless communications, why channel modeling is required, and the scope of the thesis. The motivation and objective of this thesis are also elucidated.

Chapter 2 provides a brief literature review related to the study on the local mean power estimation in different environments.

Chapter 3 discusses the measurement test equipments and briefly describes the measurement environment and measurement procedures.

Chapter 4 describes the steps of estimating local mean power and the comparison of the results observed by the measurements in this study.

Finally, a summary of the research is provided in **Chapter 5** with the concluding remarks and suggestions for future works in further research directions.

CHAPTER 2

LITERATURE REVIEW

2.1   General Background

Over the years, much research has been performed in order to model indoor channels for wireless communication systems. This chapter will briefly summarize the work performed in recent open literature, specifically as pertains to the topic of this thesis. Much attention has been paid to estimating the local mean power by adopting various methods such as:

i) window based estimators: these include the sample averaging estimator [10], [11], [12], the maximum likelihood estimator [13], and the minimum variance unbiased mean estimator [14], [15];

ii) Kalman filtering method [16], [17];

and others. However, in each technique for estimating average signal power, a local optimum was claimed based on specific frequencies, indoor/outdoor conditions, line of sight/non line of sight criteria, etc.

2.2   Studied Methods for Power Estimation

Among the studied methods, Lee's technique for estimating local mean signal power for wireless coverage is considered as the most representative and standard criteria [18]. Lee's method estimated the local mean power within a spatial interval of 20λ to 40λ where λ is the signal wavelength. A sufficient number of samples required within that

8

interval ranged from 36 to 50, and this range of samples was based on a 90 percent confidence interval and less than 1 dB error in estimation. However, there were some assumptions for this. Lee assumed that

- the signal (field) at adjacent sampled points is uncorrelated,

- small scale fading has Rayleigh amplitude statistics.

However, few queries have been raised from the above assumptions that Lee adopted:

- how does one process when the signal samples are correlated?

- how does one estimate the performance when the signal envelope obeys a distribution other than Rayleigh distribution i.e., Rician or Nakagami distribution?

The Rayleigh distribution generally presumes non-line of sight (NLOS) conditions, and Lee's study generally pertains to an urban setting. In later studies these queries were addressed by several authors along with different channel conditions, and also by considering different environments, such as, in line of sight (LOS) cases, indoor/outdoor, rural/sub-urban. In 1990, the authors in study [19] presented a conventional propagation model, including a path loss exponent, a local mean signal which follows a log-normal distribution and a fast-fading (small-scale) component in rural areas at a frequency of 900 MHz. However, attention was paid mainly on the measurement in order to determine these parameters without taking much consideration of the theoretical analysis of local mean average power estimation.

In [10], the authors studied the error statistics of real time power measurements by investigating the performance of two estimators along with the consideration of multipath and shadowing. In this investigation, they took into account a continuous time average estimator and a sample average estimator. They also considered two measurement

9

methods: filtering the squared envelope and filtering the logarithm of the squared envelope and two filter types: integrate-and-dump and RC (Resistor-Capacitor). To obtain accurate measurements, both linear and logarithmic filtering of the detected power was employed. However, they still followed the criteria proposed by Lee.

In 1997, a study [9] was also conducted on various techniques such as measured small scale fading statistics, effects of circular averaging, and linear averaging of high resolution data to characterize the accuracy of propagation prediction at 900 MHz and 2 GHz. For measured small scale fading statistics, it was observed that, the LOS small scale fading was significantly less severe than in obstructed (OBS) conditions, as expected. The depth of small scale fading approached Rayleigh statistics for heavily obstructed paths in NLOS cases. To observe the impact of the Tx and Rx antenna location, they explored the effect of circular averaging i.e., rotation of the transmitter or the receiver or both, and then compared the effect to the linear spatial averaging. The results revealed that, rotating both the dipole antennas was the most effective way to eliminate small scale fading. The study also compared the measured data with predicted ray tracing techniques in two ways: i) power sum of multipath components which was defined simply as the sum of the powers of multipath components, and ii) the vector sum of multipath components which was defined as the average of predicted powers using a large number of closely spaced points where the Radio Frequency (RF) power was proportional to the magnitude square of the vector sum of the electric field components. They observed that, the power sum ray tracing prediction technique is relatively more accurate than the vector sum technique for predicting local mean signal strength for indoor environment.

In [20], the authors analyzed the received signal using two different methods: discrete cosine transform (DCT) based data compression and robust piecewise linear approximation (RPLA). They compared experimental results with an existing filtered derivative method in order to evaluate the performance of these two methods in detecting the changes in the local mean of a signal. They tested an ideal signal with an abrupt step using DCT method and found that, the DCT method is superior to the Filtered Derivative in detecting a step change for noisy signals with signal-to-noise ratios (SNR's) as low as 7 dB. In case of the RPLA method, the authors tested two types of signals using this method, which showed that the RPLA method is capable of tracking both gradual and abrupt signal jumps for signals which have SNRs as low as 1 dB.

In 1999, Wong and Cox [14] derived the optimal local mean signal level estimator for a Rayleigh fading environment and compared with the sample average estimator. They predicted the estimation variance using the unbiased mean estimator and sample average estimator and compared those with the Cramer-Rao Lower bound. The 5th and 95th percentiles of the estimators were obtained by computer simulation. They also used Antilog Rayleigh (ALR) distribution to estimate the signal variation in a Rayleigh fading environment. It was observed that the optimum unbiased mean estimator for ALR-distributed random variables required significantly fewer samples for a given estimation accuracy compared to that of the sample average estimator.

Chai-Ko and Alouini in [15] adopted Lee's method [18], however, they considered the signal distribution over Nakagami fading channels instead of Rayleigh channels. They proposed two local mean power estimation techniques: maximum likelihood as well as minimum variance unbiased estimators. They also used Cramer–Rao

11

lower bounds similar to those Wong and Cox adopted for estimating the local mean, and confirmed that these estimators outperformed the sample mean estimator and readily approach the Cramer–Rao lower bounds. However, the difference between their study and Wong and Cox's is that Ko and Alouini assumed receiver signals with logarithmic amplification for the derivation of these estimators.

In another study [21], Avidor and Mukherjee processed the measured data to investigate the possibility of obtaining better prediction of the path loss between a mobile and the surrounding base station. They estimated the current or near future value of the local mean received power, including the shadow loss, without assuming the position or velocity of the mobile; this is different from the assumptions attempted by the other studies in [18] and [14]. They investigated the mean-squared estimation error (MSEE) as a function of the normalized speed and found that the proposed algorithm performed better than the sample mean algorithm over a wide range of mobile speeds.

De Jong and Herben in [22] adopted a two-dimensional ray tracing model for the computation of local mean power from individual multipath signals on the basis of an expression for the spatial average (SA) of the received power over each pixel area, in which they considered the spatial correlation between the signals. At larger distances from the transmitter, the method of summing all the individual ray powers no longer accurately predicts the local mean power, whereas the spatial average (SA) method provides a statistically valid approximation of the expected field strength at a random receiver position within a given observation area. They predicted that, using the SP method, the power of diffraction contributions added to the power of the direct wave resulted in an overestimation of the local mean power. The SA method handled the

contribution of diffracted ray signals to the local mean power in a correct manner, by taking into account its high correlation with the "direct" signal. They found that the SA method does not also require the calculation of the received power at many discrete points within each observation area or interval. They further indicate that poor performance of the SP method occurs particularly near the shadow boundaries associated with diffracted rays.

The authors in [13] estimated the received signal power by analyzing two techniques: the maximum likelihood estimator (ML) and median filtering technique. They compared both of these techniques along with linear filtering and a uniformly minimum variance unbiased (UMVU) estimator for power estimation. In their study, they assumed the large scale signal was constant over the duration of averaging. They observed the least mean squared error in the UMVU estimator, and found the ML estimator to be very close to the UMVU performance as the number of available data points increases. They also found that, despite the impulsive nature of the multipath process, for the same window size, the median filtering algorithm outperformed the conventional linear filter, as well as the ML and UMVU alternatives when the correlation distance was finite.

Wei and Goeckel in [23] characterized the error statistics for averaging power measurements and obtained the probability distribution of average received power on an "outdated" measurement. By comparing various models, they also derived a number of novel power control algorithms to compute the estimation error and demonstrated that the power control algorithm based on their expression can minimize the average transmitted power required to achieve a desired outage probability.

The authors in [16] proposed a novel Kalman-Filter-based estimator for the local mean power on the basis of a first-order autoregressive (AR) model of the shadowing process assuming that the shadowing process is constant over the duration of the averaging window. They compared the Kalman-Filter-based estimator with various window-based estimators: sample average (SM) estimator, the uniformly minimum variance unbiased (UMVU) estimator, and the maximum likelihood (ML) estimator. They showed that the window-free KF either meets or exceeds the performance of conventional window-based causal estimators and observed that a relatively small sampling period yields better least square error (LSE) performance for Kalman filter (KF). However, they assumed the mean of the log-normal fading to be zero, and the variances of both the small scale and the large scale fading to be known. The path loss and the correlation coefficient between consecutive samples were also assumed to be known. The KF is also generally more complex to implement than the other methods.

Osorio and Huerta in [8] implemented an experimental technique to calculate the variation of the local mean power in an indoor environment at two different frequencies: 900 and 1900 MHz. They also developed a comparison of the large scale fading estimates for the calculation of total quadratic (mean-square) error with the consideration of three factors: the distance-dependent average path loss, the variation in the local mean power, and the small-scale fading. The experimental technique for estimating local average power were demonstrated as SA technique. However, this technique (i.e., dividing the walk route into intervals and then averaging the samples of the received power in each interval) is similar to the window based sample average estimator proposed by prior authors.

In order to constrain the effect of fast fading on the statistical value of the signal within ± 1 dB, the statistical interval was estimated to be *larger* than 40λ in a separate study by Lin et al. [24]. However this technique is to some extent different from the result proposed by Lee [18], in that averaging a segment of signal data with a length longer than 40λ risks smoothing out the long-term fading information. Therefore, too long a statistical interval may smooth out not only small scale fading information, but also the large scale fading information one is trying to estimate.

In 2006, the authors in [25] extended the Kalman filtering approach proposed in another study [16] to adaptive Kalman filtering by combining the Kalman filtering with the window based filtering and showed that the proposed method outperforms the window-based approaches and eliminates the Kalman filter's parameter requirements. They found that a much smaller number of samples is required when compared to the median (by sorting the samples and taking the median value) case. For a standard deviation of 1 dB, 25 samples were required in the Kalman case, whereas it was 36 for the window based approach [18], resulting in a 30% decrease in the number of samples. The difference between the study of [16] with adaptive Kalman filtering is that the static Kalman filter provided the performance results for the case when all the parameters were exactly known.

La Vega et al. in [11] generalized Lee's method for their analysis of the signal variability and proposed an algorithm to find the channel parameters. The authors studied determination of proper values of the parameters defined by the original method proposed by Lee, but made the process independent from the propagation channel, the frequency band and the reception conditions. They proposed a new methodology for obtaining the

"*2L*" parameter (physical averaging length) and followed the same procedure for the number of samples (*N*) and sampling interval (*d*) parameters as described by Parsons and Lee. For the parameters *2L* and *N*, they obtained considerably smaller values ($2L = 2.1\lambda$, $d = 0.17\lambda$ and $N = 8$ samples) than those obtained by Lee and Parsons. This was due to the relationship between wavelength and the size of the obstacles that generated variations in the long-term signal, and in the case of *N*, to the lower signal variability in the medium wave AM broadcasting (MW) band, especially in rural and suburban environments.

Jiang et al. [26] also analyzed Lee's criteria in more detail. They modified the standard Lee method for estimating local mean signal power by considering the correlation relationship to compute the covariance between different sample points, the mutual influence between statistical interval and sampling interval. However, there are some problems in their derivation:

➢ Considering only the neighboring samples to be correlated may be incorrect, since this can yield much higher variance errors.

➢ They also proposed that, the longer the length of the statistical interval, the smaller the statistical error. However, most of the researchers on this topic demonstrated that, the longer the length of statistical interval, the more likely it is to smooth out the large scale fading characteristics, which causes an incorrect local mean estimation if the length of statistical interval is over some maximum length.

In 2011, the authors in [12] established novel statistical criteria for obtaining the parameters proposed by Lee by adopting two more factors into consideration: confidence

level and the number of measurement runs. They also proposed an evaluation equation to determine the lower and upper bounds of the statistical interval. They established the following results:

➢ There is no necessity for the sampling points to be uncorrelated.

➢ The upper and lower bounds of the statistical interval are not limited to be within 20λ to 40λ. The range can be larger than 40λ and smaller than 20λ. They considered 30λ to be appropriate in most conditions, but this is not true in every condition.

Jadhavar and Sontakke in [27] presented different propagation models within an indoor environment. They took measurements at 2.4 GHz using two different multi-storied buildings, which included wall partitions, a number of floors and different building layouts. They proposed their study in modeling first order prediction of distance dependent mean signal strength inside a building. However, their models are only suitable for a particular type of building and there is no theoretical basis for their models.

In 2014, Pappas and Zohdy in [17] proposed an Extended Kalman filter (EKF) method to optimize the shadow power state estimation. They developed an accurate estimation of parameters, higher order state space prediction methods and an Extended Kalman filter (EKF) for modeling shadowing power in wireless mobile communications. Path-loss parameter estimation models were compared and evaluated and then compared to existing Kalman Filter (KF) methods with Gaussian and non-Gaussian noise environments and they established a conclusion that the Extended Kalman Filtering performs significantly better than Kalman Filtering at the expense of larger estimation complexity.

17

What has not been thoroughly covered in the literature is specification of the estimation parameters ($2L$, N_{min}, and d_{min}) for LOS settings, in either indoor or outdoor environments. Our work in this thesis addresses this gap for an indoor setting.

CHAPTER 3

EQUIPMENT AND EXPERIMENTAL PROCEDURES

3.1   Equipment Description

In this thesis, a signal generator was employed as a transmitter (Tx) and a spectrum analyzer was used as a receiver (Rx) in order to measure received signal power. A frequency of 5.725 GHz was used for both the transmitter and the receiver. This was selected as it is a common band used for wireless local area networks (WLANS). The frequency span was set to 200 kHz, so as to measure only our transmitted signal of interest, and no other (extraneous) signals. The resolution bandwidth of the spectrum analyzer was set to 100 Hz in order to reduce the background noise, i.e., select only our transmitted signal. In subsequent sections, the equipment used for the measurements is briefly discussed.

3.1.1   Signal Generator

The signal generator is a type of electronic test equipment that can generate multiple types of repeating or non repeating electronic signals. These test sets are also sometimes known as function generators, RF and microwave signal generators, etc. For this measurement, an Agilent N51821A signal generator (Figure 3.1) was employed, which has the following major characteristics:

  ➢ Frequency range of 100 kHz to 6 GHz

➢ ≤ +23 dBm output power up to 3 GHz using a highly-reliable, fast-switching electronic attenuator

➢ ≤ 900 μs simultaneous frequency, amplitude, and waveform switching in list mode.

Figure 3.1 Agilent N51821A Signal Generator.

3.1.2 Spectrum Analyzer

A spectrum analyzer measures the power of an input signal as a function of frequency within the full frequency range of the instrument. The spectral distribution of power of all received signals (e.g., known and unknown) can be measured. The display of a spectrum analyzer has frequency on the abscissa and the power (usually in a logarithmic, dB, scale) displayed on the ordinate. An Agilent N9342C spectrum analyzer (Figure 3.2) was employed, which has the following major characteristics:

➢ Total frequency range of 9 kHz to 7 GHz

➢ Amplitude accuracy of ±1.5 dB

➢ < 0.4 s sweep time for 7 GHz full span

Figure 3.2 Agilent N9342C Spectrum Analyzer.

3.1.3 Antennas

Two Mobile Mark DM2-5500 Omni-directional quarter wave monopole antennas were used for the transmitter (Figure 3.3) and the receiver (Figure 3.4). The transmitter and the receiver antennas were placed on two equipment carts at the same elevation of 1.5 m above the floor. The antennas are also covered by plastic radomes. A RZ-214 cable was used to connect the transmitting antenna to the signal generator and the losses of the cables were approximately 3.8 dB. Both the transmitter and the receiver have ~1.3 dB antenna gain as characterized by the manufacturer. These antenna gains are the measure of the antenna's radiation efficiency defined as the ratio of the maximum radiation in a given direction to that of a reference (isotropic) antenna for equal input power. The antennas were vertically polarized. Figure 3.5 shows the antenna pattern for the DM2-5500.

Figure 3.3 Mobile Mark DM2-5500 Transmitter (Tx) Antenna (within white radome) mounted in cardboard box atop equipment cart.

Figure 3.4 Mobile Mark DM2-5500 Receiver (Rx) Antenna, with extended ground plane, atop cardboard box and wooden board on cart.
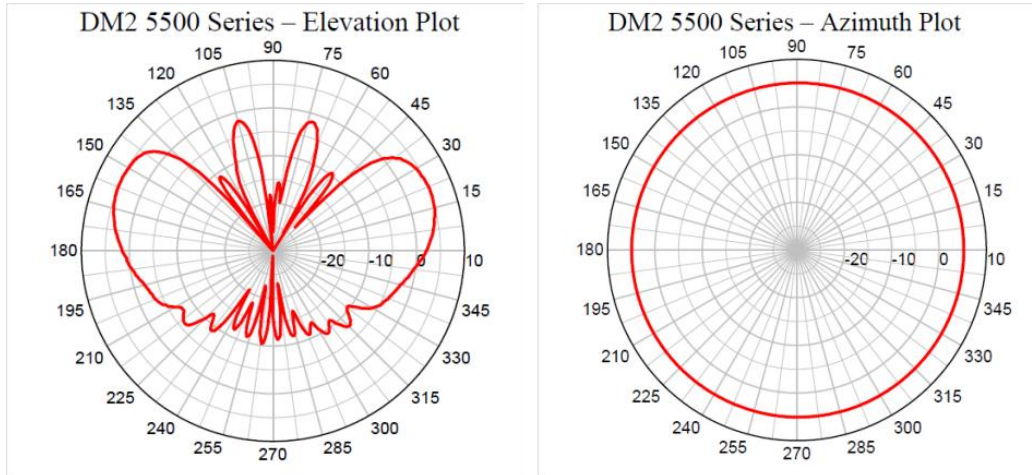
Figure 3.5 Antenna patterns for DM2 5500.

3.2   Measurement Procedure

The measurements for radio propagation were conducted along the hallway of the "D" wing in the second floor of Swearingen Engineering Center at the University of South Carolina on September 23rd, 2014. The main goal was to measure and then model the propagation path loss in this example indoor environment. The measurements were taken in a LOS environment without any blockages between Tx and Rx. A number of explicit distances were pre-marked with respect to the stationary Tx location along the hallway in order to position the Rx.

3.2.1   Experimental Set Up and Procedure for Indoor Hallway Environment

First the Tx signal generator (SG) was set up on a cart and configured to have a sine-wave output at a frequency of 5.725 GHz and a transmit power of 17 dBm which was the maximum power for the signal generator. The SG was powered with AC (alternating current) and connected to the Tx antenna. RF connectors were also aligned carefully before tightening. Figure 3.6 shows the set up for the signal generator.
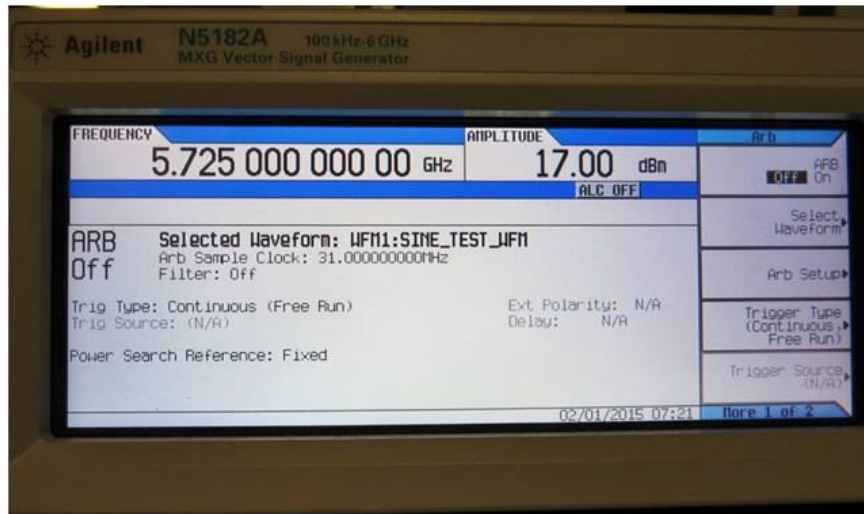
Figure 3.6 Signal generator set up on the Tx side.

The measurement set up parameters for the signal generator are shown in Table 3.1. After setting the SG as the Tx, the transmitting antenna was placed at a fixed position (centered) in the far end of the hallway (Figure 3.7).

Table 3.1 Measurement set up parameters for the Signal Generator

Measurement set up	
Carrier frequency (GHz)	5.725
Resolution Band width (Hz)	100
Transmit power (dBm)	17
TX antenna height (m)	1.5
RX antenna height (m)	1.5
Cable Loss	3.8

Figure 3.7 Transmitter Antenna set up.

In order to average out the small scale fading effects, data (received power in dBm) was taken at specific link distances (from d_{L1}=4.57 m to d_{L9} = 41.15 m) along the hallway. At each link distance, the Rx antenna was moved from the left point to the right point along an "arc" that represents the constant value of link distance. A conceptual diagram of this whole procedure and also a portion of the Swearingen second floor plan is shown in Figure 3.8.
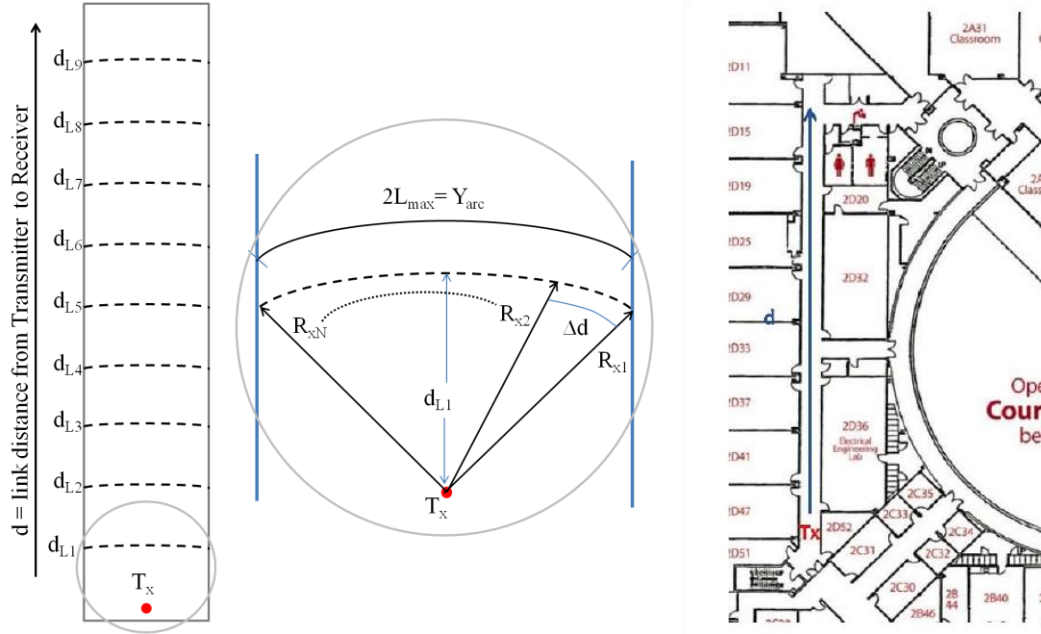
Figure 3.8 A conceptual diagram of measurement procedure along with geometric parameters is on the left, a portion of the Swearingen second floor plan is on the right.

As indicated in Figure 3.8, the receiver antenna was fixed at each point along the arc at each link distance for 10 seconds to collect a set of received power samples. For example, at a link distance of 4.572 m, a total number of 220 data files was collected, where each file represents a number of received samples at a given Rx antenna position. In each file, approximately 75 to 85 samples were taken in 10 seconds at each of the 220 antenna positions. The separation interval between each antenna position (the measurement points), denoted Δd, was 1 cm, or slightly less than $\lambda/5$ (where the wavelength, $\lambda = c/f = 3\times10^8$ m/s$/5.725\times10^9$ Hz = 5.24 cm). Figure 3.9 shows a photograph of the Rx antenna position at 4.57 m, with the Tx antenna fixed at the far end of the hallway.

Figure 3.9 Position of Rx Antenna.

As an example, the received amplitude of -54.35 dBm measured by the spectrum analyzer at a distance of 4.57 m away from Tx, for one measurement point, is shown in Figure 3.10.
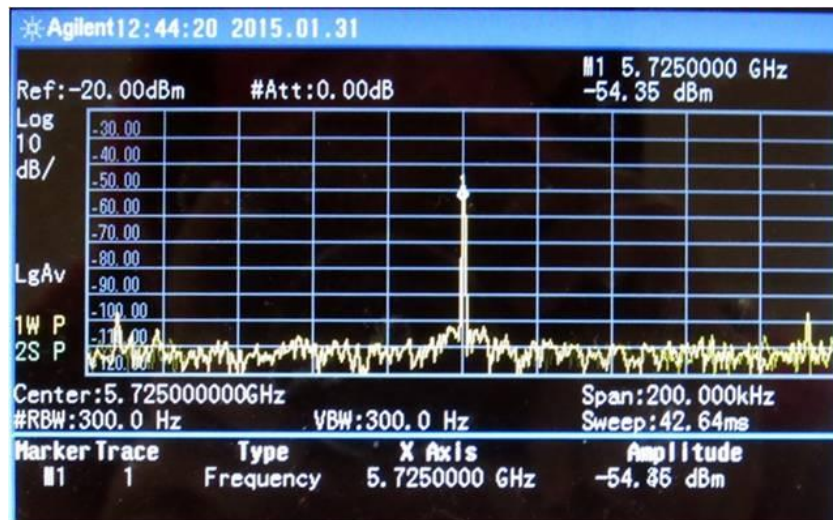

Figure 3.10 Received Power when Rx at a link distance of 4.57 m.

A large number of received power values were collected at each distance along the hallway (e.g., 220 at $d = 4.57$ m). Received power values at nine different distances (from 4.57 m to 41.15 m at an interval of 4.57 m) were collected to evaluate the path loss as well as estimate the local average power. The path between transmitter and receiver was carefully monitored and measured data were collected in the condition where there was no obstacle obstructing the LOS.

CHAPTER 4

ANALYSIS, RESULTS AND DISCUSSIONS

4.1   Theoretical Analysis

As mentioned in section 1.3, there are three major channel characteristics that are important in modeling an indoor wireless channel: path loss, small-scale fading (multipath), and shadowing (local mean power variation). In this section, a brief discussion about these channel characteristics is provided.

4.1.1   Path Loss Model

Usually shadowing or large-scale fading characteristics of any radio channel are determined by measurements of the path loss (*PL*). Path-loss values in dB are computed using the following link budget equation.

$$PL = P_t + G_t + G_r - L_t - L_r - P_r \qquad (4.1)$$

In (4.1), P_t is the transmitter power in dBm, G_t and G_r are, respectively, the Tx and Rx antenna gains in dB, L_t and L_r are the RF cable losses at Tx and Rx, in dB, and P_r is the local mean received power in dBm. Experimental path-loss data can be used to construct a path-loss model. In realistic indoor mobile radio channels, a widely used model, defined as the log-distance path loss model, is often used, which is as follows (in dB),

$$PL(d) = PL(d_0) + 10nlog\ (d/d_0) + X_\sigma \qquad (4.2)$$

In (4.2), *PL(d₀)* is the path loss in dB at a reference distance d_0 in m, and *n* is the dimensionless path loss exponent, which is obtained by fitting this one-segment model to the measured path loss samples. X_σ is a zero mean Gaussian distributed random variable of standard deviation σ which accounts for effects such as shadowing (by obstacles of sizes generally much larger than a wavelength), or in LOS cases, the average deviation of measurements from the linear model of the first two terms of equation (4.2). Figure 4.1 shows the log-distance path loss model for the D-wing corridor in the building of Swearingen Center (second floor), University of South Carolina, along with the measured path losses prior to estimating the local mean power.
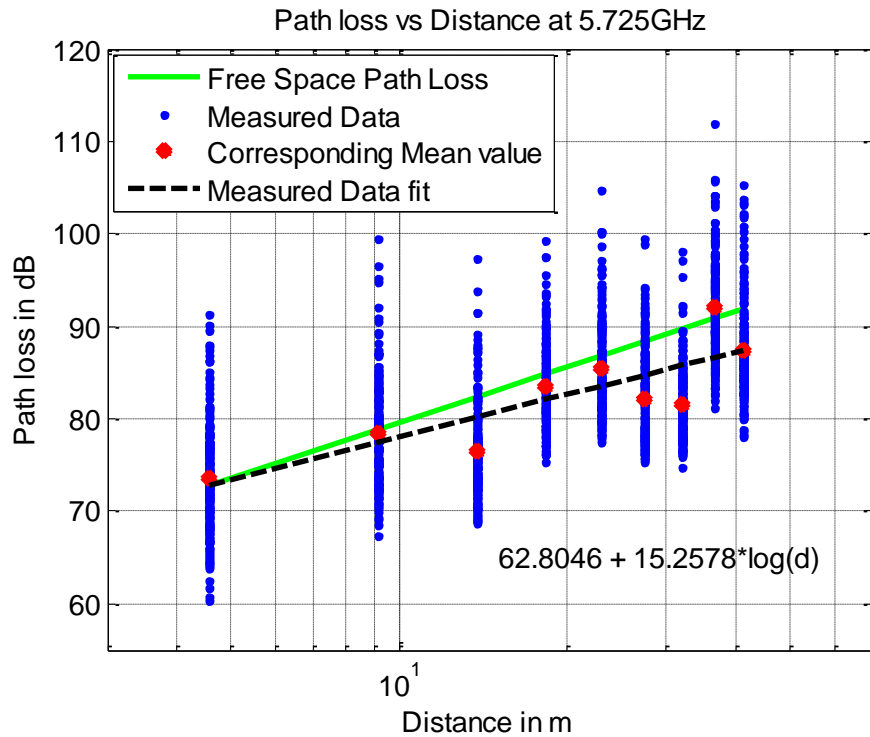

Figure 4.1 Path loss model for indoor corridor in Swearingen Center (second floor), University of South Carolina, with all measured values at nine different link distances from 4.57 m to 41.15 m.

From linear fit in Figure 4.1, it was found that the path loss at the reference distance of 1 m was 62.8 dB, the path loss exponent was 1.52, and the standard deviation was 5.66 dB. As expected in this corridor environment, a wave guiding effect of the corridor walls, floor, and ceiling yields a mean path loss that increases with distance less than in free space.

4.1.2 Steps for Local Mean Power Estimation

The main objective of this thesis was to estimate the local mean received power P_r to obtain an accurate path loss model. To estimate the local mean, we assumed a widely accepted model for the received signal amplitude in the following product form:

$$r(y) = m(y)r_0(y) \qquad (4.3)$$

In equation (4.3), y is the distance along an arc at a constant value of link distance [Figure 3.8], r is the total received amplitude, m is the large-scale fading and r_0 is the small-scale fading amplitude which is obtained by dividing the received instantaneous signal amplitude r by the estimated local means. In the following subsections, the important parameters for estimating local mean values are discussed.

4.1.2.1 Determining the Averaging Interval *2L*

In an indoor environment, the variation of the large scale signal is an important factor to be considered for obtaining an accurate estimation of local mean power by determining an appropriate averaging interval *2L*. As proposed by the author in [18] (for outdoor, NLOS environments), the estimation of the local mean power is obtained by measuring over intervals of length in the range of 20 to 40 wavelengths, and then the samples are averaged inside each interval. However, this criteria might not appropriate for the case of indoor environments, particularly in the LOS case. An appropriate

averaging interval *2L*, is that which is large enough to average out the small scale fading, but small enough so as not to smooth out the large-scale fading.

Our approach is described as follows (and will be clarified via the pertinent equations and an example). The calculation of the optimum range for *2L* is based on amplitude segments of measured field strength samples, i.e., the received signal envelope *r(y)* mentioned above. For each segment, the estimated local means were computed by way of their running means. These estimated mean values were then normalized to the corresponding total mean values over the arcs at fixed link distance. Once the estimated means values were normalized by the approximate true mean values, the spread of the set of those normalized mean values was evaluated by computing their standard deviation. In the LOS, the variation of the large scale effect might be less than that of the small scale effects, and it is hence of most interest to obtain only the lower limit of the averaging window length (*2L*) range.

By considering different window sizes, the following steps are used to determine an appropriate value of *2L*; as noted, this value should be large enough to eliminate the small scale fading, but small enough so as not to smooth out the large-scale fading. For a total of *N* amplitude values across the arc (at fixed link distance), select a test value of window length *S* (corresponding to *2L*).

➢ *Compute*

$$s_j = \sum_{i=i_j}^{i_j+S-1} \frac{r_i}{S} \quad , \; i_j = 1,2,\ldots K = N - S + 1\;; \qquad (4.4)$$

32

In equation (4.4), s_j is the window-length-S mean amplitude, where the i_j are the starting indices of each window, and a length-K vector of local (window-spanning) means $\underline{s}=[s_1,\ s_2,\ ...s_K]$ results.

➤ *Compute*

$$r_{norm,\,j}= s_j / \sum_{k=1}^{K} \frac{s_k}{K}\ ; \tag{4.5}$$

In equation (4.5), the $r_{norm,j}$ are the normalized window-length-S means or the normalized running means, i.e., to get a local value of $2L$, each window-spanning mean s_j is normalized with respect to the corresponding mean of the s_j values across the entire arc at a given value of link distance.

➤ *Compute*

$$1\sigma_{r\_spread} = 20\ log\frac{(1+\sigma_{r\_norm})}{(1-\sigma_{r\_norm})}\ ; \tag{4.6}$$

In equation (4.6), σ_{r_norm} is the standard deviation of the normalized running means $r_{norm,j}$, and $1\sigma_{r\_spread}$ is the spread in logarithmic scale (dB), both for the given test values of S and N.

Repeat these steps for additional values of S (hypothesized values of $2L$).

➤ Finally, for obtaining the optimal length of $2L$, Lee's criterion was adopted, which is based on the condition that the 68% of the estimated mean values fall within a range of 1 dB around their true mean. That is, the optimum value of $2L$ is when $1\sigma_{r\_spread} = 1$ dB or smaller. This algorithm is illustrated in Figure 4.2 with a simple example.
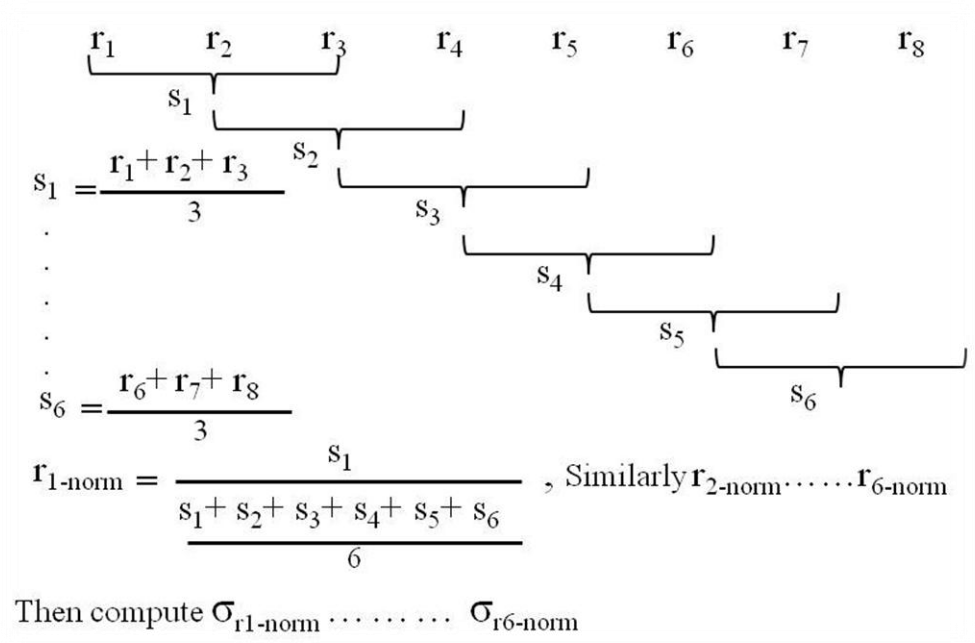
Figure 4.2 Illustration of algorithm computation steps, for $N = 8$, $S = 3$.

The window size S was varied from 0.38λ to 41.79λ to see the variation of sigma spread. Here, 41.79λ is the window length over the entire set of N samples (the arc length for each link distance), i.e., if $K = N-S+1$, where N = total number of samples = 220, S = window size = 220 then the sigma spread will go to zero.

4.1.2.2 Determining Minimum Separation d_{min} between Uncorrelated Samples

After obtaining values for (the minimum of) $2L$, it is necessary to know the minimum separation d_{min} between two adjacent samples by computing the autocorrelation among those samples. One of the important step consists of normalizing the samples, because the variation of the local means along the arc distance influences the autocorrelation coefficient. The estimate of parameter d_{min} will enable validation of the

34

2L value. If the distance relative to the autocorrelation first null is less than 0.2, the samples will be considered uncorrelated.

To obtain d_{min}, the received amplitude for a specific window length was considered. For example, if *N* samples r_1 through r_N are obtained from a measurement track with a specific averaging window *2L*, then the normalized autocorrelation function *RXX (S)* associated with that track is calculated as [28]:

$$R_{XX}(S) = \frac{\sum_{k=1}^{N-S}(r_{k+S})r_k}{\sum_{i=1}^{N} r_i^2} \qquad (4.7)$$

4.1.2.3 Determining Minimum Number of Samples N_{min} within an Optimum *2L* Interval

After determining *2L* and d_{min}, the parameter N_{min} can be obtained by the following equation (4.8),

$$N_{min}\, d_{min} = 2L \qquad (4.8)$$

N_{min} will be sufficient within *2L* if it also satisfies the condition [5] in equation (4.9), which involves a Gaussian assumption regarding the estimation error. In (4.9), *m* and σ_r are the approximate true mean and the true sigma of S_j, respectively for the calculated optimum window length, *2L*. This inequality also implies that the maximum error should fall within a range of ± 1 dB around the estimated true mean, *m*.

$$20log_{10}(m + 1.65\frac{\sigma_r}{\sqrt{N_{min}}}) - 20log_{10}(m - 1.65\frac{\sigma_r}{\sqrt{N_{min}}}) \le 2 \text{ dB} \qquad (4.9)$$

4.2   Analysis of Simulated Data

To test the performance and accuracy of the local mean estimation algorithms, we created a computer simulation. Note that, ultimately we are using *measured* data for our evaluations; the simulation simply allows us to gain insight into the algorithm operation.

The small scale amplitude, $r_0(y)$ and the large scale signal, $m(y)$ were generated using a Rayleigh distribution and a simple sinusoidal function, respectively, and the functions were multiplied to generate the signal envelope $r(y)$. Figure 4.3 shows a histogram of generated small scale signal samples which fits well by the Rayleigh probability density function (pdf).
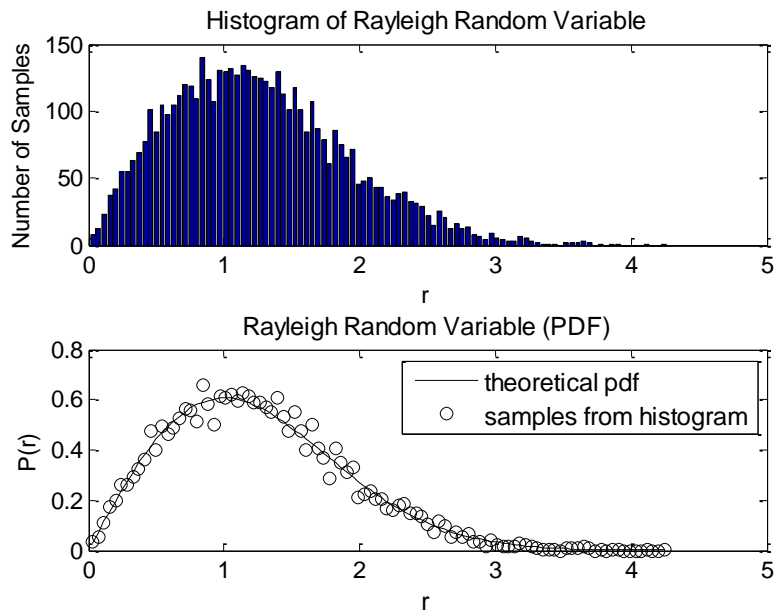

Figure 4.3 Small scale signal generation: histogram of generated Rayleigh random variables compared to the theoretical pdf.

The signal envelope $r(y)$ was generated for 5000 random samples. Figure 4.4 shows a small segment of 500 samples of the signal envelope along with the small scale signal and the large scale signal. Figure 4.5 shows normalized small scale field signal strength $r_0(y)$ in dB.
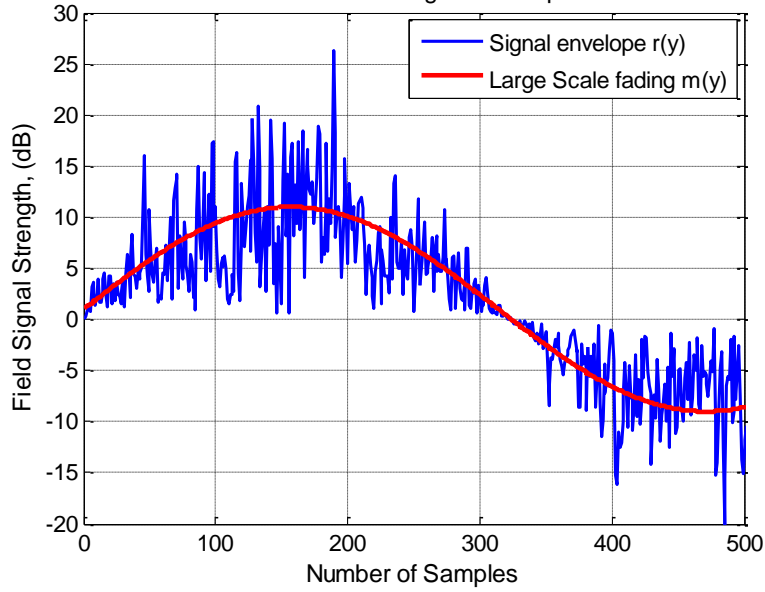
Figure 4.4 Received signal envelope and large-scale component as a function of sample number.
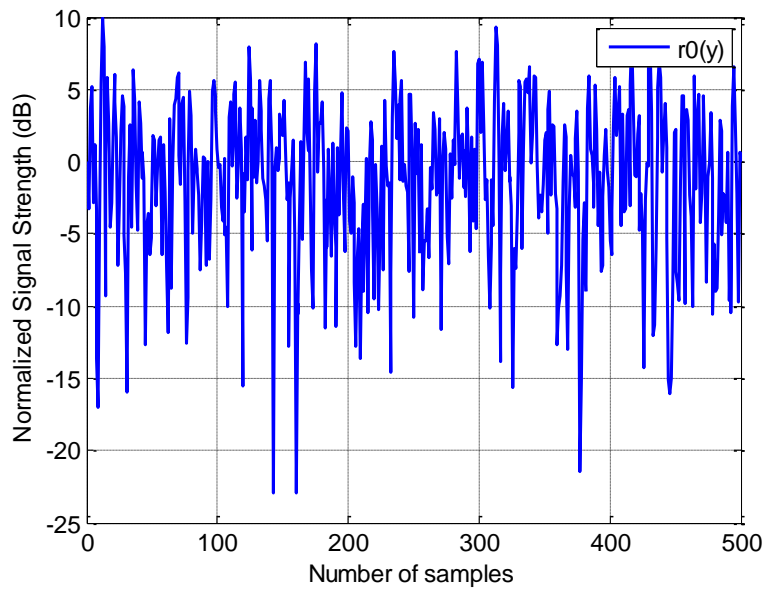

Figure 4.5 Normalized small scale fading amplitude as a function of sample number.

We applied the algorithm to the simulated received signal envelope for 500 samples with varying window sizes *2L* (averaging window). As can be observed from Figure 4.6, the spread of sigma essentially monotonically decreased. As we are interested

in the minimum value of *2L* such that the spread is < 1 dB, the minimum value appears as

2L = 24λ.
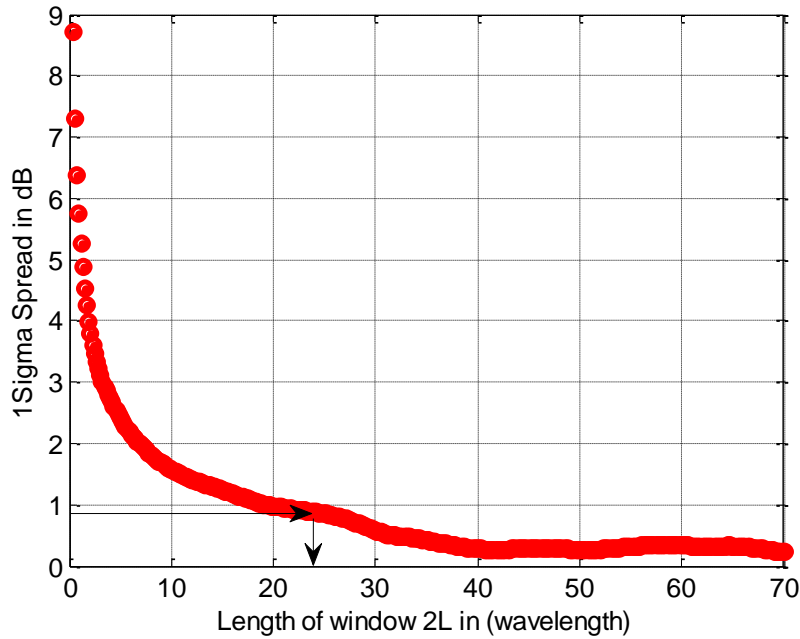
Figure 4.6 One-sigma spread vs. averaging window length *2L*, for 500 simulated samples. One-dB threshold indicated by arrows.

The minimum separation between two neighboring points (d_{min}) was calculated using the equation 4.8. From Figure 4.7, the minimum separation or the sampling distance was calculated as d_{min} = 14/5.24 = 2.67λ which is larger than the theoretical value (d_{min} = 0.5λ) found by Lee [14]. Yet this is to be expected since this is a LOS environment: the spatial field is dominated by the LOS component. Thus using equation 4.7, the required number of samples N_{min}=2L/d_{min}= 24λ/ 2.67λ = 9 samples.
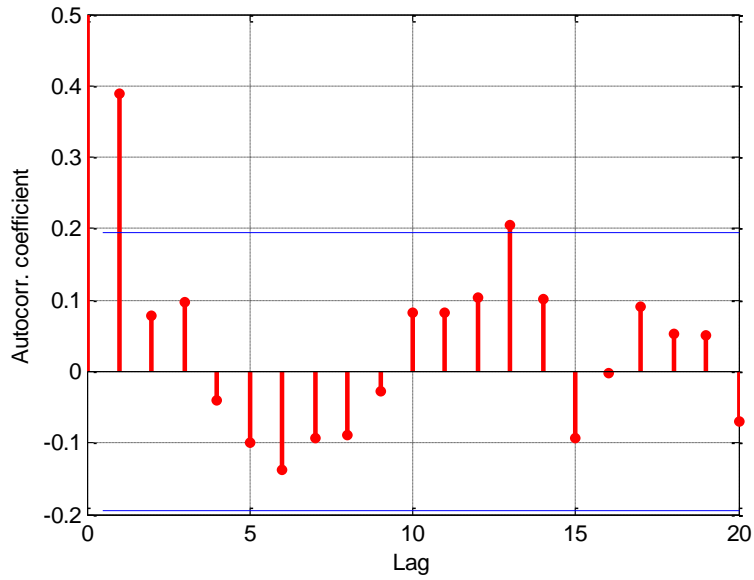
Figure 4.7 Autocorrelation coefficient for obtaining d_{min}.

The algorithm was also applied for a set of 220 simulated sample points since the total number of measurement points was 220. In this case, the spread goes below 1dB at $2L = 15\lambda$ which is shown in Figure 4.8. Therefore, the required number of samples for 220 points was calculated to ($N_{min} = 2L_{opt}/d_{min} = 15\lambda/2.67\lambda$) 6 samples.
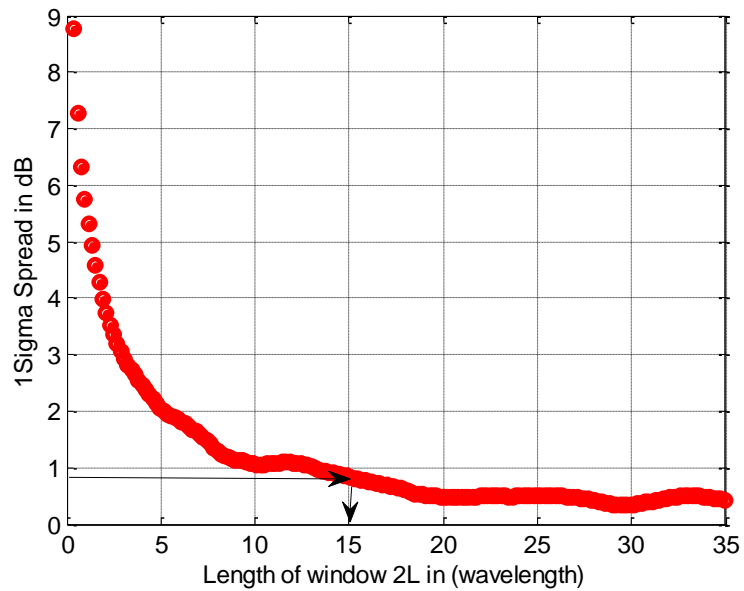

Figure 4.8 One-sigma spread vs. averaging window length $2L$, for 220 simulated samples. One-dB threshold indicated by arrows.

4.3   Analysis of Measured Data

As mentioned in Chapter 3, the measurement data was acquired for nine different values of link distance along the hallway to compute the spread of sigma vs. the averaging window length. The following sub-sections show plots of $1\sigma_{r\_spread}$ as a function of $2L$ at each link distance from 4.57 m to 41.15 m.

4.3.1   Rx Position of 4.57 m

It can be observed from Figure 4.9 that, the optimum averaging interval $2L$ at a point of sigma spread < 1 dB was obtained as 35λ at d_{L1} = 4.57 m. The d_{min} was calculated as 13/5.24 = 2.48λ using Figure 4.10. After obtaining $2L$ and d_{min}, the required number of samples within the averaging window of length $2L$ was calculated using equation 4.8, which is $N_{min} = 35\lambda/2.48\lambda = 15$ samples.
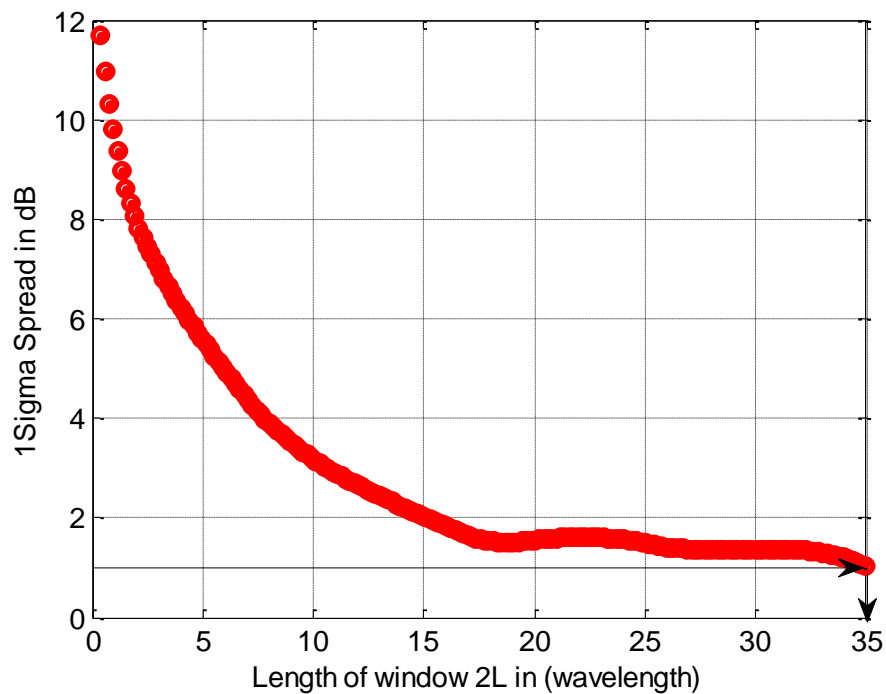

Figure 4.9 Spread of estimated local means as a function of $2L$ when d_{L1} was 4.57 m. One-dB threshold indicated by arrows.
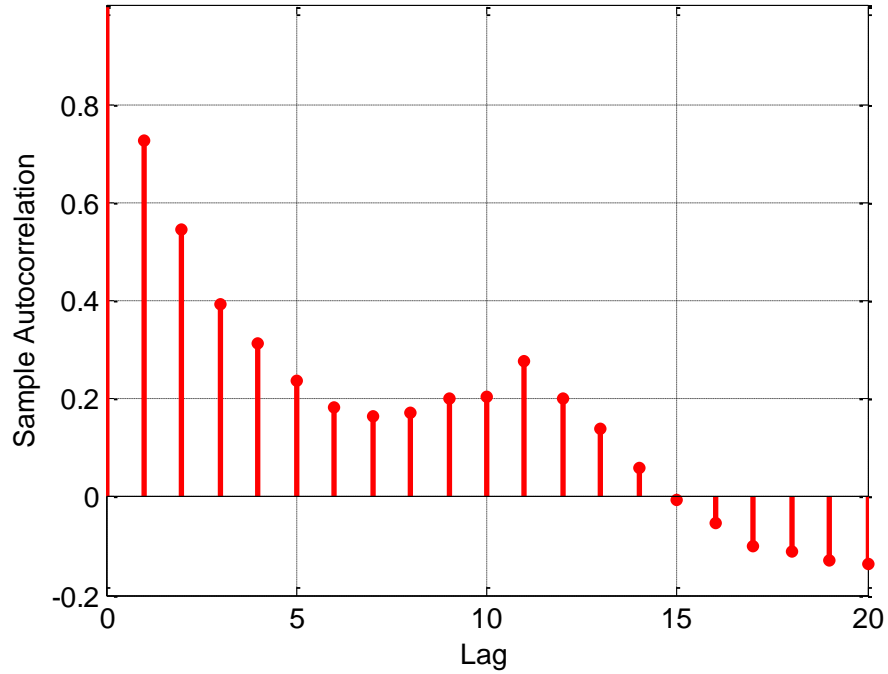
Figure 4.10 Autocorrelation coefficient within a specific *2L* interval.

Figure 4.11 illustrates the received signal envelope along with the estimated large scale signal, $m(y)$ using the calculated optimum window length, $2L = 35\lambda$. It can be seen that $m(y)$ is nearly constant (within ~1 dB) for index values 50 to 110, and within around 2 dB for index values 50-150 in the hallway center. As the local mean is expected to be exactly constant across the arc of the hallway—since the link distance is a constant, our estimate of $m(y)$ confirms this. Variation of the local mean near the walls is also expected, as an "edge effect".
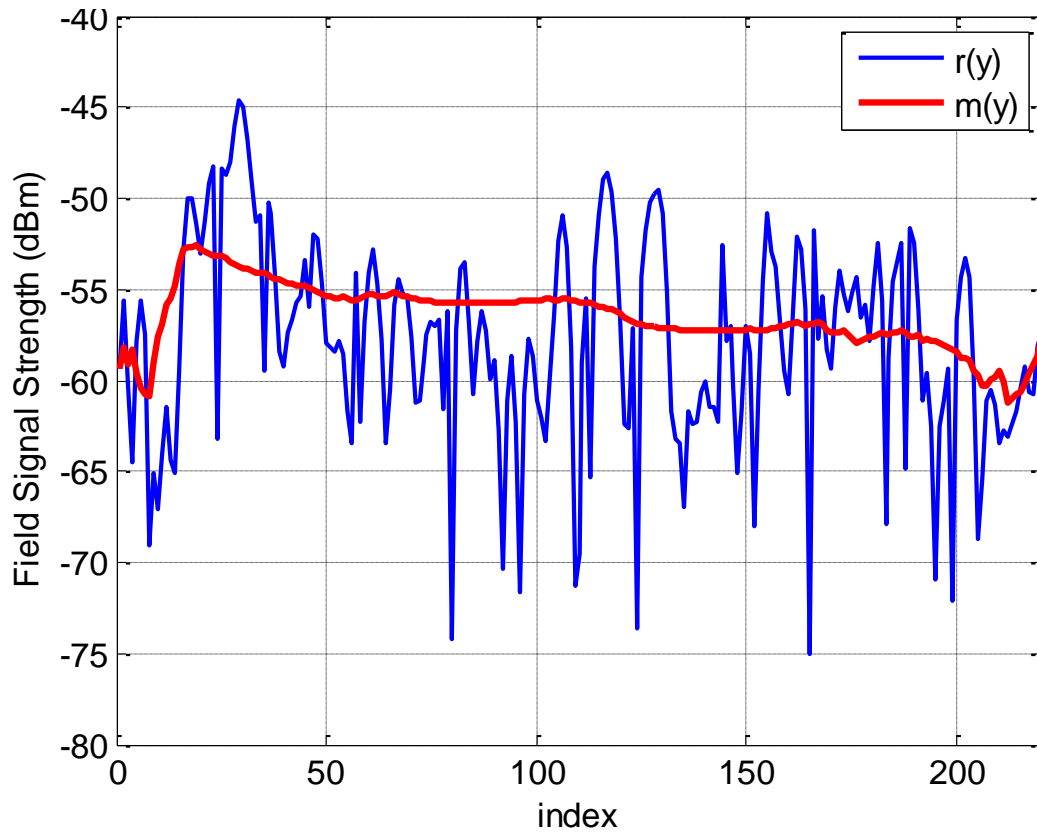
Figure 4.11 Signal envelope using optimum averaging window length at $d_{L1} = 4.57$ m.

4.3.2 Rx Position 9.144 m

At the link distance of 9.144 m, the spread of sigma as a function of optimum averaging length was computed, and is presented in Figure 4.12.
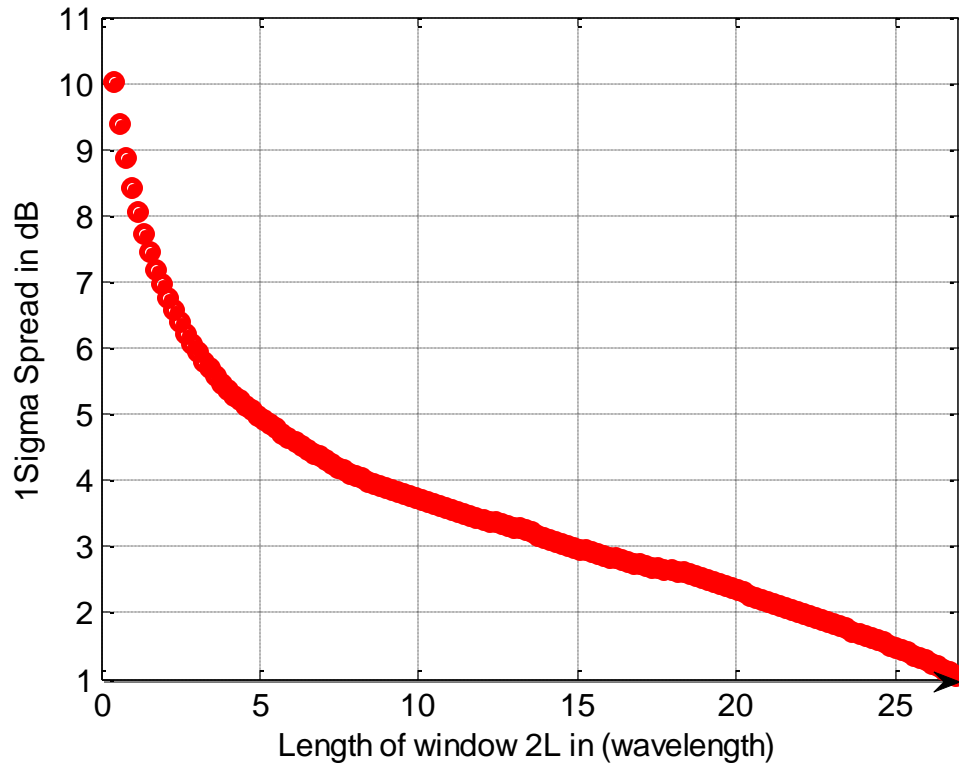
Figure 4.12 Spread of estimated local means as a function of *2L* when d_{L2} was at 9.144 m. One-dB threshold indicated by arrows.

The optimum window length *2L* was obtained from Figure 4.12 as 28λ. Note that, at each link distance, the sampling interval d_{min} did not vary much and therefore the most frequent value of d_{min} was considered as 2.48λ. It again can be observed from Figure 4.13 that *m(y)* was roughly constant (within ~1 dB) for index values 95 to 150, and within around 2 dB for index values 60-150 in the hallway center.
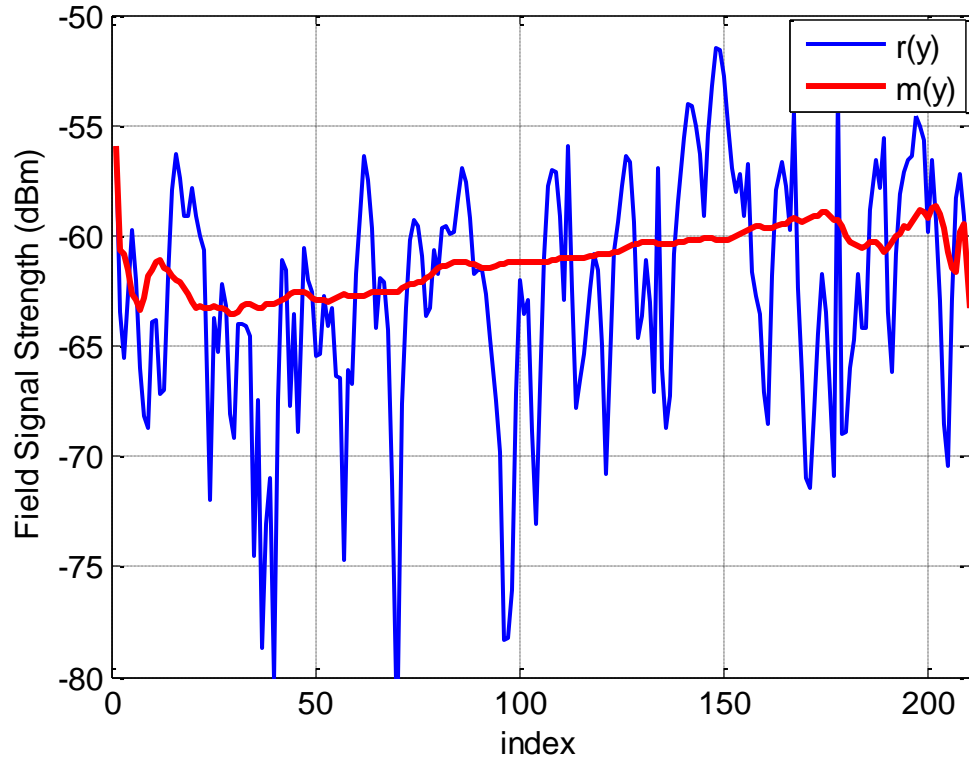
Figure 4.13 Signal envelope using optimum averaging window length at d_{L2} = 9.14 m.

4.3.3   Rx Position 13.72 m

For this value of link distance, the optimum window length *2L* was obtained as

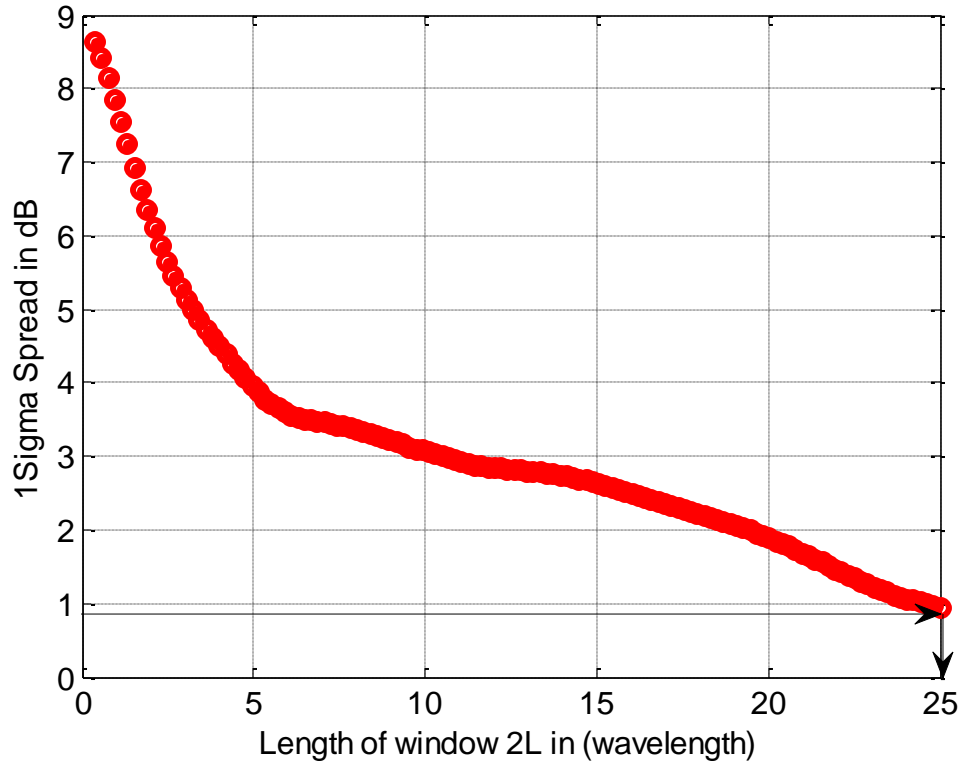25λ at the point of sigma spread ~ 1 dB or less, showing in Figure 4.14.

Figure 4.14 Spread of estimated local means as a function of $2L$ when d_{L3} was at 13.72 m. One-dB threshold indicated by arrows.

The received signal envelope using the optimum length, $2L = 25\lambda$, is shown in Figure 4.15 where, once more, $m(y)$ is roughly constant (within ~1 dB) for index values 80 to 150, and within around 2 dB for index values 60-150 in the hallway center.
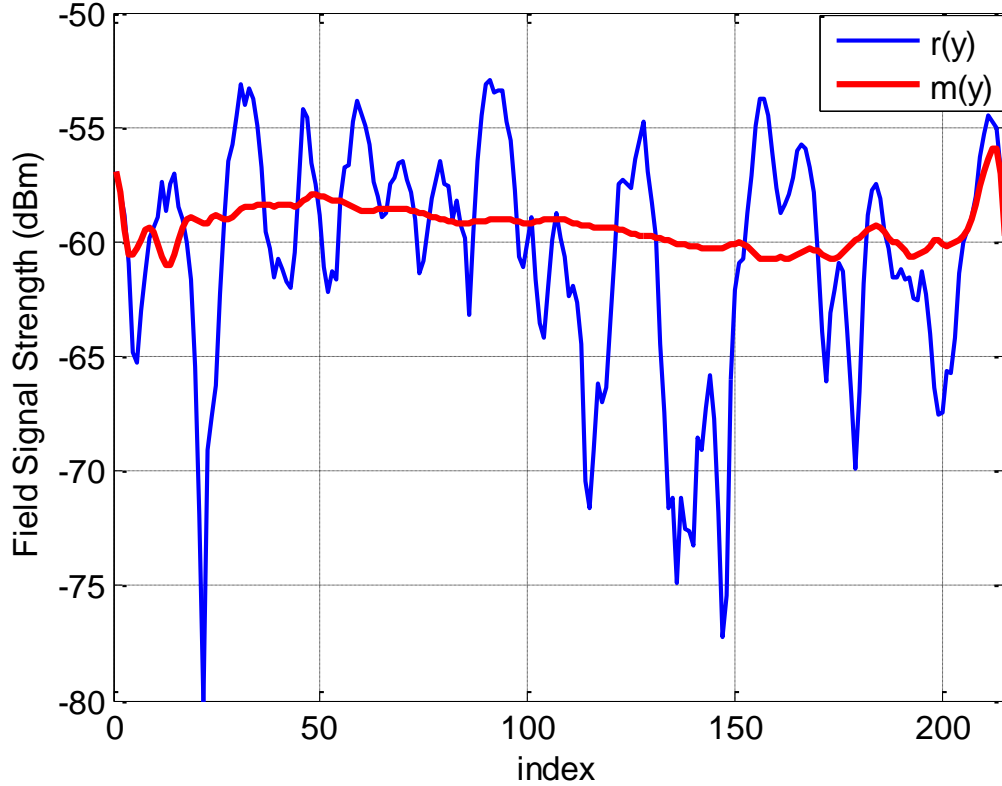
Figure 4.15 Signal envelope using optimum averaging window length at d_{L3} = 13.72 m.

4.3.4 Rx Position 18.28 m

For the 18.28 m link distance, $2L = 21\lambda$ as observed from the Figure 4.16. The received signal envelope using the optimum length, $2L = 21\lambda$, is shown in Figure 4.17 and as at smaller values of link distance, it was found that $m(y)$ is approximately constant (within ~1 dB) for index values 50 to 110, and within around 2 dB for index values 50-170.
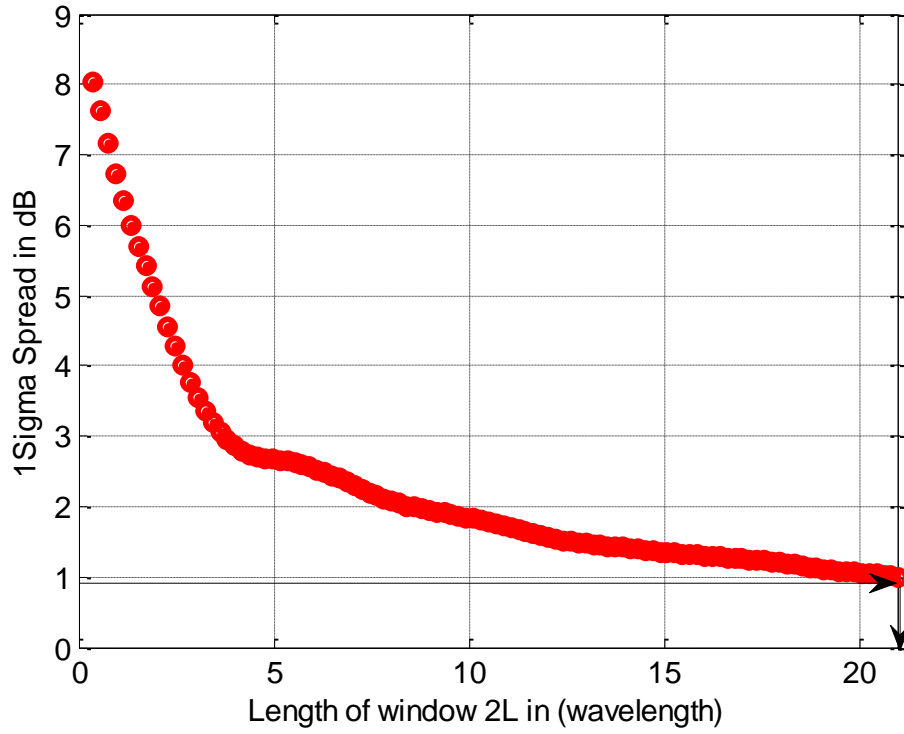
Figure 4.16 Spread of estimated local means as a function of *2L* when d_{L4} was 18.28 m.
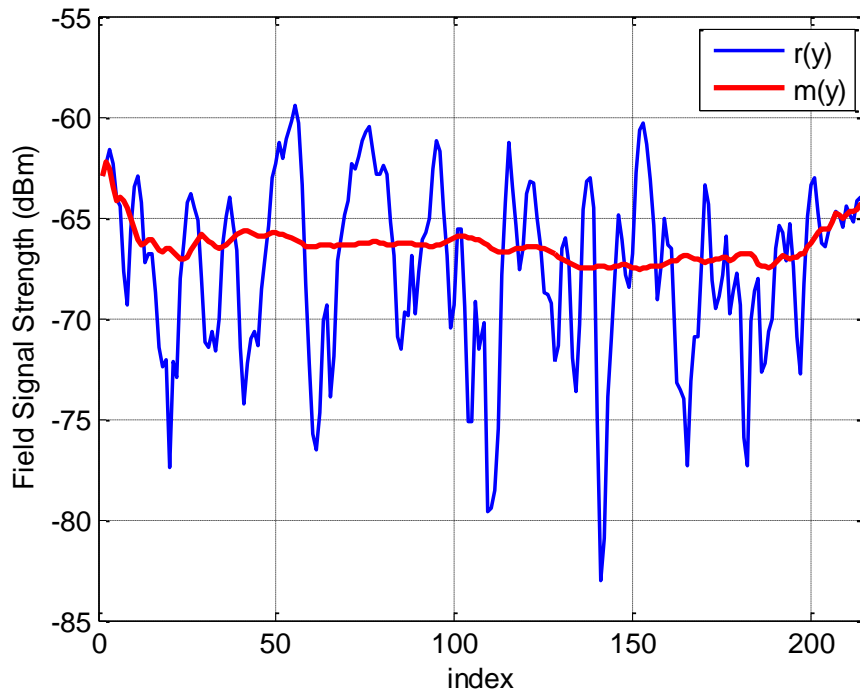One-dB threshold indicated by arrows.

Figure 4.17 Signal envelope using optimum averaging window length at d_{L4} = 18.28 m.

4.3.5 Rx Position 22.86 m

For the 22.86 m Rx position, the averaging window length was slightly larger than the value observed from figure 4.18. In this case, $2L = 26\lambda$. The received signal envelope using the optimum length, $2L = 26\lambda$, is shown in Figure 4.19. It can be observed again that $m(y)$ is roughly constant (within ~2 dB) for index values 50 to 160.
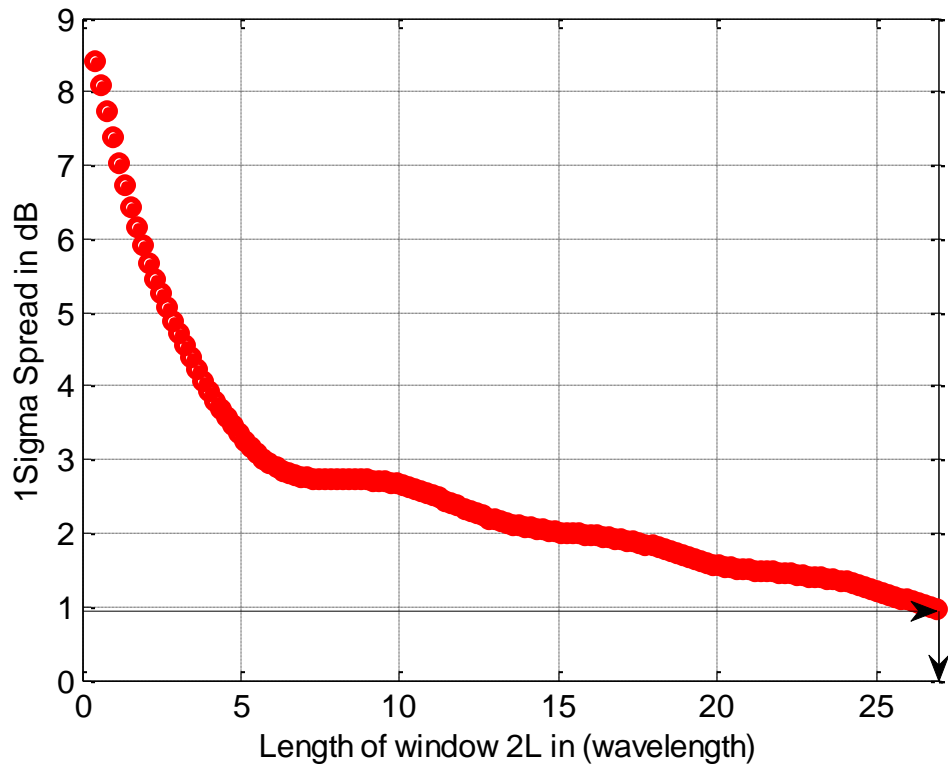

Figure 4.18 Spread of estimated local means as a function of $2L$ when d_{L5} was 22.86 m. One-dB threshold indicated by arrows.
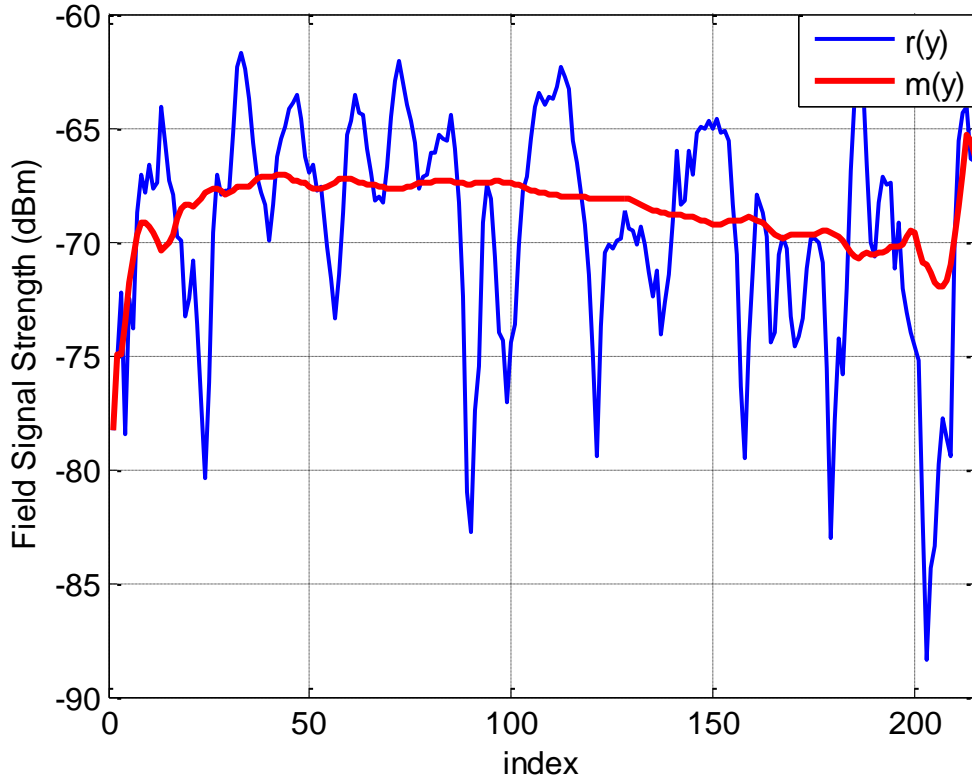
Figure 4.19 Signal envelope using optimum averaging window length at $d_{L5} = 22.86$ m.

4.3.6   At Rx position 27.43 m

At the 27.43 m Rx position, *2L* was found to be 24λ, as shown in Figure 4.20. The received signal envelope using this optimum length, *2L* = 24λ, is shown in Figure 4.21. Here, *m(y)* is again roughly constant (within ~2 dB) for index values 50 to 150 exactly in the hallway center.

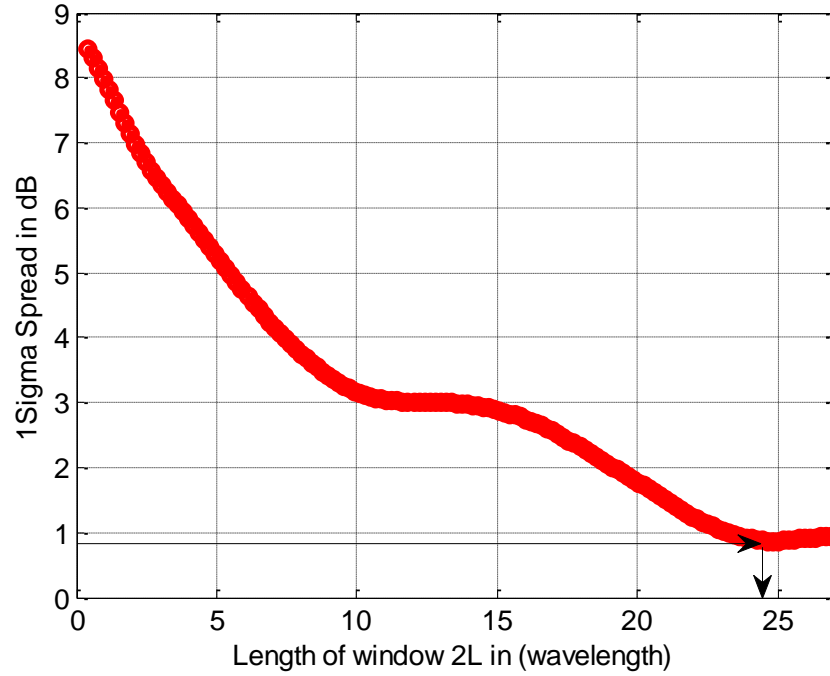Figure 4.20 Spread of estimated local means as a function of *2L* when d_{L6} was 27.43 m. One-dB threshold indicated by arrows.
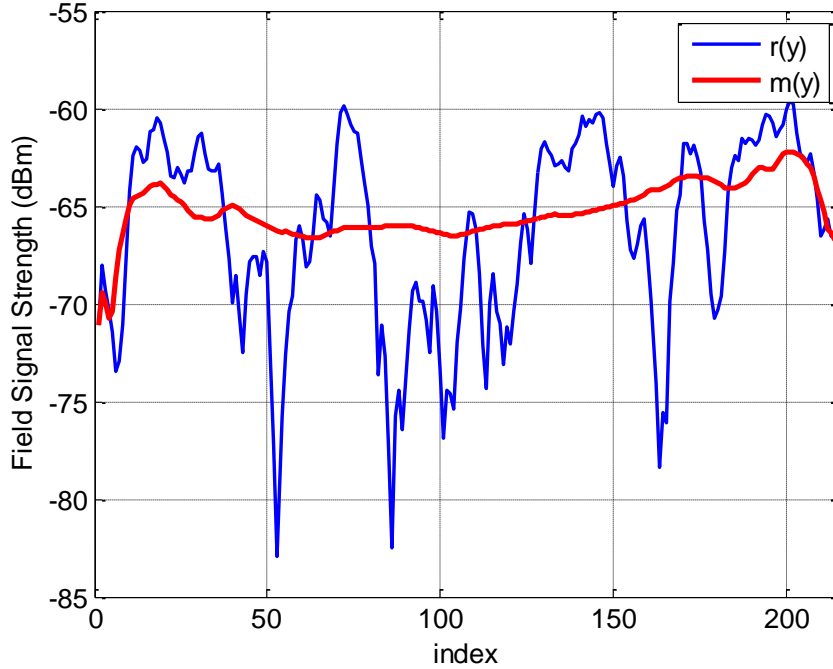

Figure 4.21 Signal envelope using optimum averaging window length at d_{L6} = 27.43 m.

4.3.7 Rx Position 32 m

From Figure 4.22, at this link distance, the optimum window length was found as $2L = 8\lambda$.
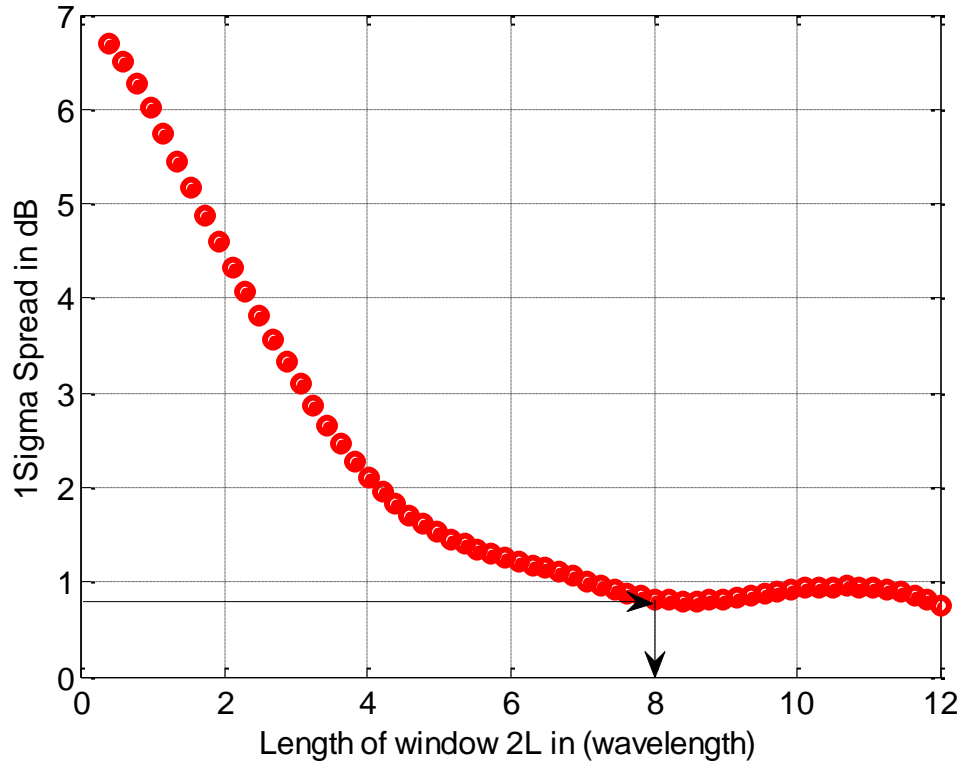

Figure 4.22 Spread of estimated local means as a function of $2L$ when d_{L7} was 32 m. One-dB threshold indicated by arrows.

To get the minimum number of samples within the averaging window, corresponding $d_{min=}8/5.24=1.53\lambda$. The normalized autocorrelation coefficient was observed as 8, shown in Figure 4.23 since if we consider the most frequent value of $d_{min=}$ 2.48λ, the minimum number of samples resulted to $N_{min} = 4$ samples which is not consistent with prior results. The received signal envelope using the optimum length, $2L = 8\lambda$, shown in Figure 4.24. As we might expect, with this relatively small value of window length, the local mean is not quite as "flat" as for the prior link distances with

larger values of window length. Nonetheless, the local mean variation is still ~ 2 dB over the majority of the width of the hall. Worth pointing out is that for this link distance, another corridor extends perpendicularly from ours (see Fig. 3.8), allowing for more spatial field variation.
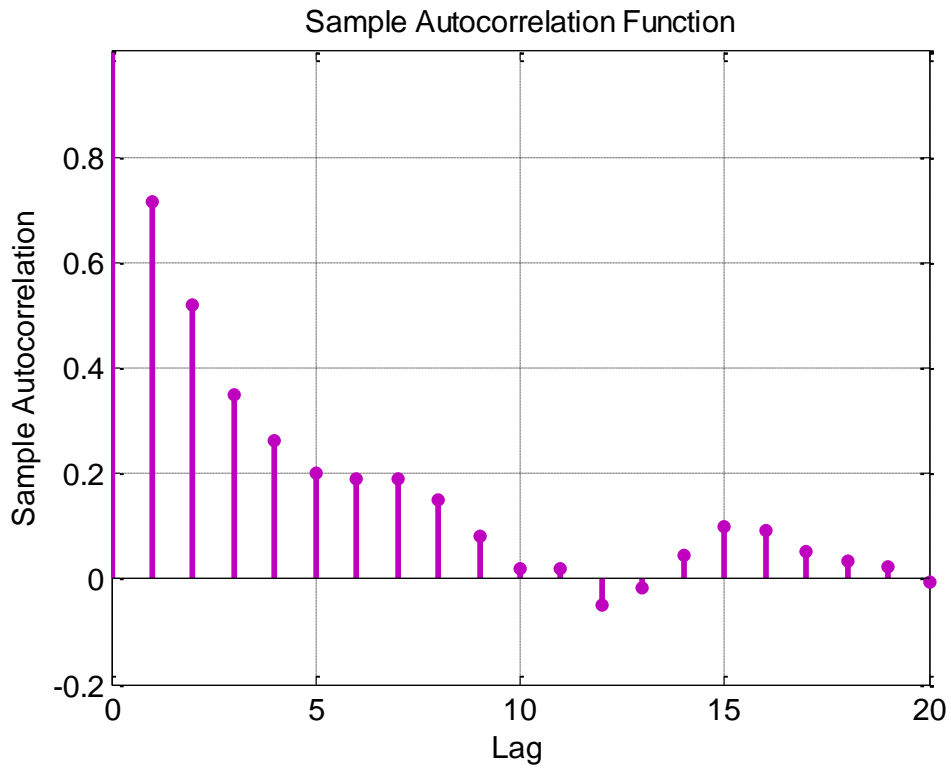

Figure 4.23 Autocorrelation coefficient within a specific *2L* interval.
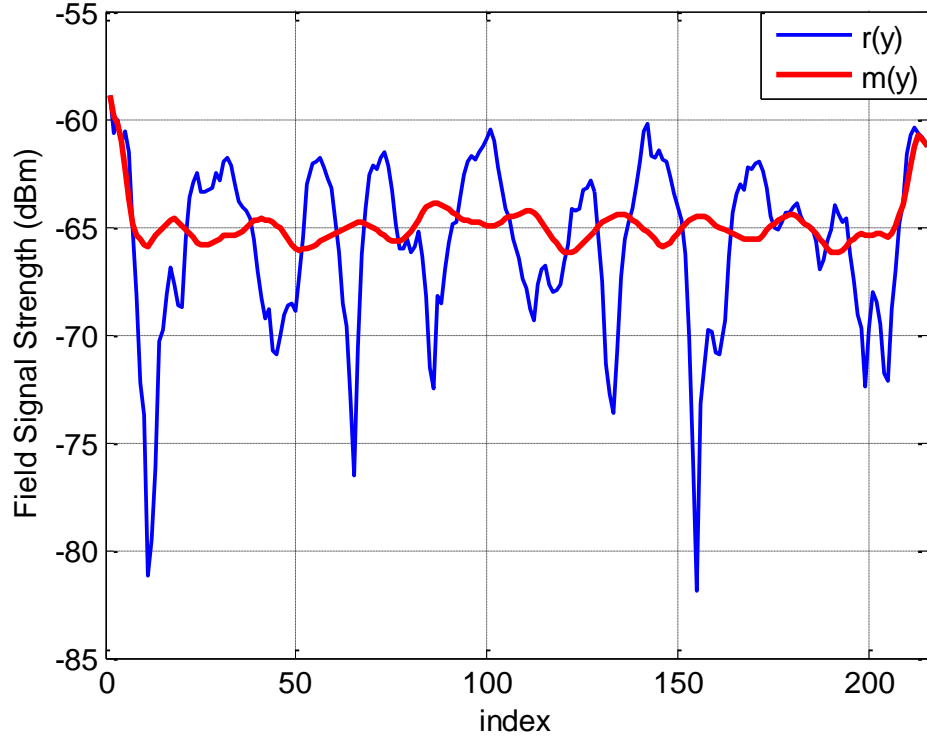
Figure 4.24 Signal envelope using optimum averaging window length at $d_{L7} = 32$ m.

4.3.8 Rx Position 36.58 m

Similarly Rx position at 36.58 m, the optimum averaging window from the Figure 4.25 was, $2L = 33\lambda$ and the required number of samples was, $N_{min} = 13$ samples while $d_{min} = 2.48\lambda$. The received signal envelope using the optimum length, $2L = 33\lambda$, as shown in Figure 4.26. Here once again, $m(y)$ is roughly constant (within ~2 dB) for index values 50 to 120 exactly in the hallway center, although there is a noticeable slight downward trend from left to right. This effect would be a subject for future analysis.

Figure 4.25 Spread of estimated local means as a function of *2L* when d_{L8} was 36.58 m. One-dB threshold indicated by arrows.
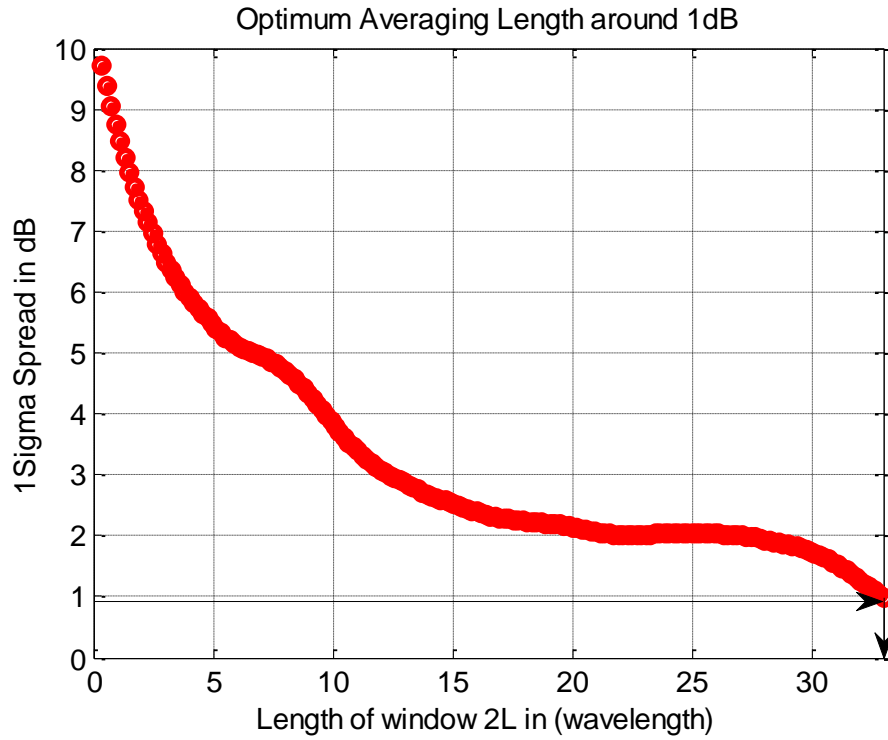

Figure 4.26 Signal envelope using optimum averaging window length at $d_{L8} = 36.58$ m.

4.3.9   Rx position 41.15 m

From Figure 4.27, the optimum window length for our maximum value of link distance was, $2L = 27\lambda$. The autocorrelation coefficient for this link distance is shown in Figure 4.28 and the received signal envelope using the optimum length, $2L = 27\lambda$, as shown in Figure 4.29. As in the previous cases, $m(y)$ is approximately constant (within ~1 dB) for index values 60 to 140 in the hallway center.

Figure 4.27 Spread of estimated local means as a function of $2L$ when d_{L9} was 41.15 m. One-dB threshold indicated by arrows.

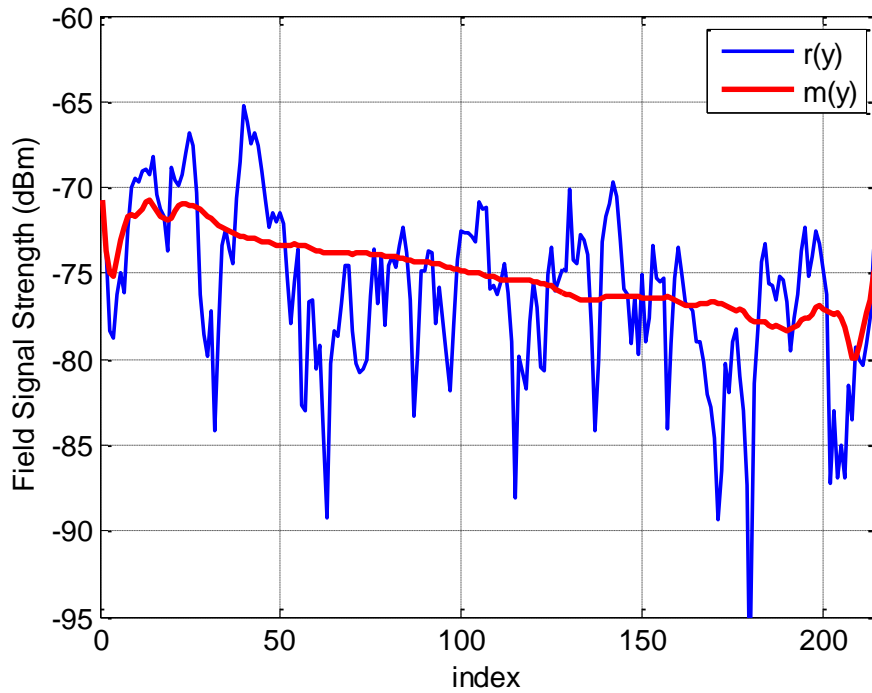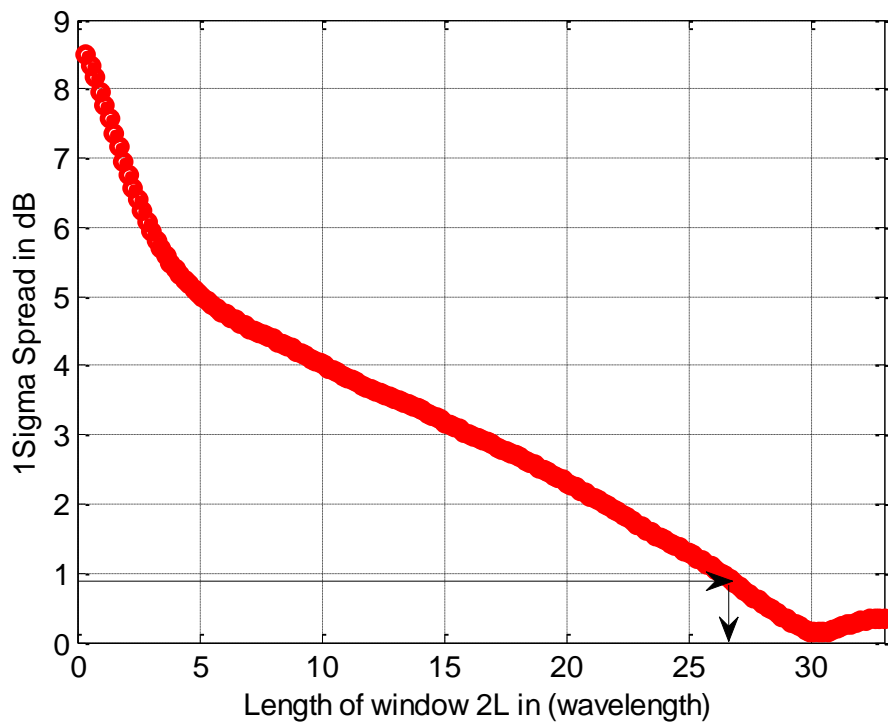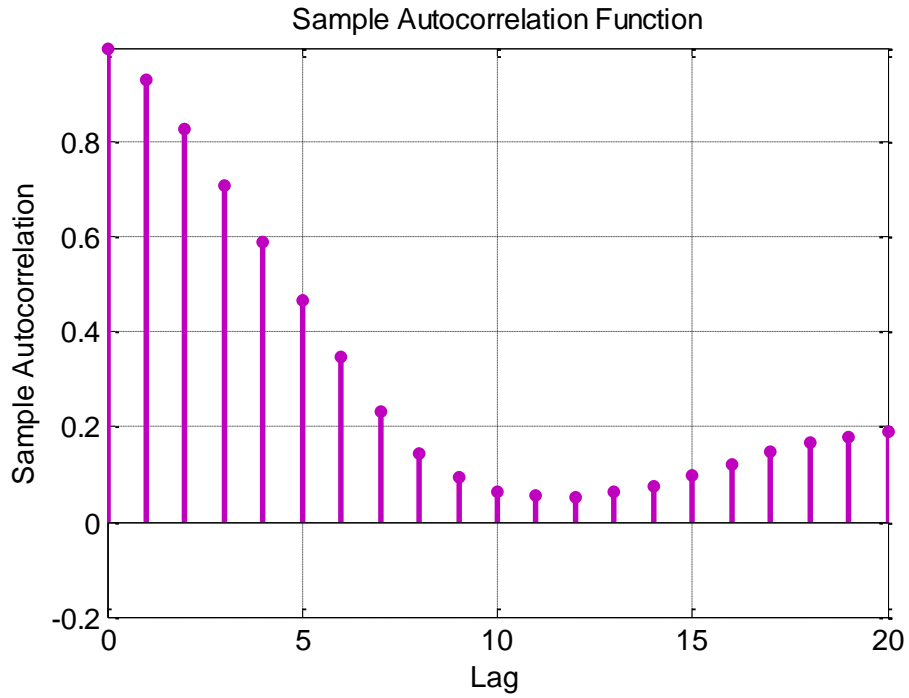Figure 4.28 Autocorrelation coefficient within a specific *2L* interval.
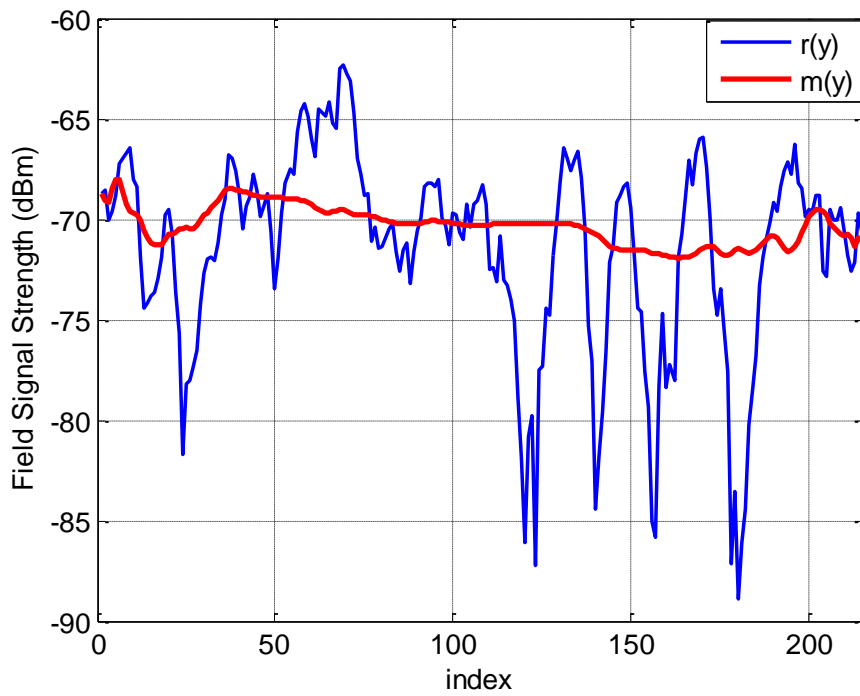
Figure 4.29 Signal envelope using optimum averaging window length at $d_{L9} = 41.15$ m.

The sampling distance vs. the calculated window length at each link distance is shown in Figure 4.30 where the most frequent value for d_{min} (its mode) was found to be 2.48λ; this value was used to determine the required number of samples within the averaging window at each link distance. To be most conservative with d_{min}, we *could* select the maximum value of 4λ. Similarly, the most conservative (maximum) value of N_{min} is 15, so using (4.8), $2L = 15 \times 4\lambda = 60\lambda$ would be the most conservative value of $2L$, which is here unnecessarily large, almost twice the largest value of $2L$.
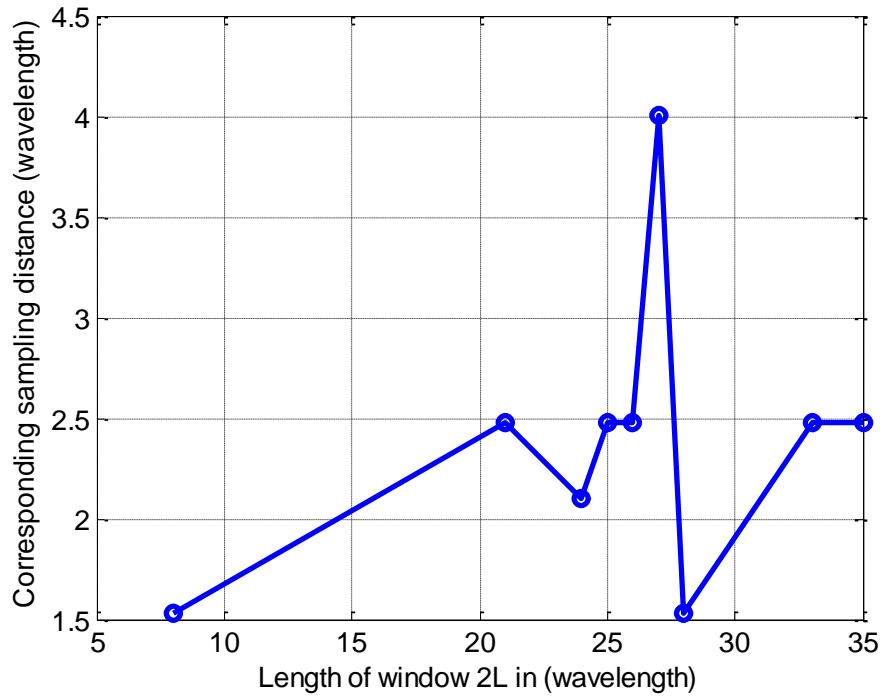
Figure 4.30 Calculated sampling distance vs. window length.

Figure 4.31 shows the plot of averaging window length $2L$ as a function of link distance. Up to the distance of ~31 m, the window length generally decreases with link distance. Table 4.1 summarizes the values of $2L$, d_{min}, and N_{min} for all the link distances from 4.57 m to 41.15 m.
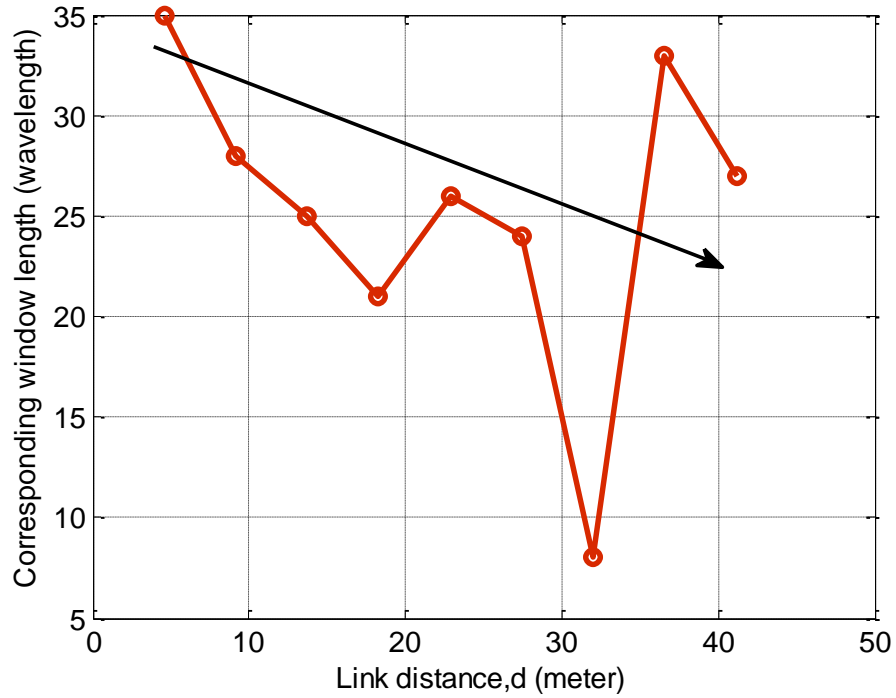
Figure 4.31 Calculated averaging window length *2L* as a function of link distance, *d*.
Trend line with distance also shown.

Table 4.1 Values of *2L*, d_{min} and N_{min} for nine different link distances

Link Distance (m)	Values of *2L* (wavelengths)	d_{min} (wavelengths)	N_{min} (samples)
4.57	35	2.48	15
9.14	28	1.53	12
13.72	25	2.29	10
18.29	21	2.48	9
22.86	26	2.48	11
27.43	24	2.09	10
32.00	8	1.53	6
36.58	33	2.48	13
41.15	27	4.00	11

Therefore, over the range of studied link distances, the window length *2L* decreased from 35λ to 8λ with increasing link distance, although the decrease was not exactly monotonic, and the 8λ value is likely anomalously small. As for N_{min} (which decreased from 15 to 6 samples), we might expect it to also monotonically decrease with link distance if we had a perfectly smooth and uniform corridor, since that would produce strong waveguiding beyond some moderate value of link distance. This did occur for the first four of nine distances, but N_{min} increased slightly for the link distance of 22.86 m and also for the largest two values of link distance, 36.58 m and 41.15 m. The reason for this is hypothesized to be the inhomogeneity of the environment, e.g., the corridor has doors and a few hallways extending from the side of the corridor near the Rx positions at 36.58 m and 41.15 m.

CHAPTER 5

CONCLUSIONS AND FUTURE WORK

5.1   Concluding Remarks

The main objective of this study was to obtain the parameters required to estimate the local average power in line-of-sight (LOS) indoor settings at a frequency of 5.725 GHz. The estimation of the local mean power in an indoor environment and some effects of the local mean variations were presented. The pivotal parameters for estimation are the spatial averaging window length, the spatial separation between two neighboring sample points, and the number of samples within that window length. These parameters were themselves estimated at different link distances with a fixed transmitter location. The method of sample average estimator was applied to the measurement data, and also to an example set of simulated fading data.

For the measured data analysis, the averaging window length (2L) was found to be between 8λ - 35λ . We found the minimum number of samples (N_{min}) to be 6 to 15 samples, and the sample separation (d_{min}) to be 1.53λ to 4λ. For our measured data set, the window length decreased monotonically until a link distance of 22.86 m and also for the largest two of the link distances, 36.58 m and 41.15 m, respectively. Our hypothesis for this increase is that the structure of the hallway becomes quite irregular at these larger values of link distance .

5.2   Future Work

In the future, this study could be further developed and extended to different corridors, in different LOS indoor settings. Measurements in different frequency bands would also be of interest. The algorithms themselves should be further studied and refined as well. It could be also interesting to see the effect of moving the mobile unit or receiver unit from outdoor to indoor or indoor to outdoor settings to study how the local mean power estimation would need to be modified.

REFERENCES

[1]   A. F. Molisch, *Wireless communications*: John Wiley & Sons, 2007.

[2]   A. Goldsmith, *Wireless communications*: Cambridge university press, 2005.

[3]   T. S. Rappaport, *Wireless communications: principles and practice* vol. 2: Prentice Hall PTR New Jersey, 1996.

[4]   G. L. Stüber, *Principles of mobile communication*: Springer Science & Business Media, 2011.

[5]   J. D. Parsons and P. J. D. Parsons, "The mobile radio propagation channel," 1992.

[6]   D. W. Matolak, "Channel modeling for vehicle-to-vehicle communications," *Communications Magazine, IEEE,* vol. 46, pp. 76-83, 2008.

[7]   I. Sen and D. W. Matolak, "Vehicle–vehicle channel models for the 5-GHz band," *Intelligent Transportation Systems, IEEE Transactions on,* vol. 9, pp. 235-245, 2008.

[8]   J. Sesena-Osorio*, et al.*, "Experimental estimation of the large-scale fading in an indoor environment and its impact on the planning of wireless networks," in *Microwave & Optoelectronics Conference (IMOC), 2013 SBMO/IEEE MTT-S International*, 2013, pp. 1-5.

[9]   R. A. Valenzuela*, et al.*, "Estimating local mean signal strength of indoor multipath propagation," *Vehicular Technology, IEEE Transactions on,* vol. 46, pp. 203-212, 1997.

[10]   A. J. Goldsmith*, et al.*, "Error statistics of real-time power measurements in cellular channels with multipath and shadowing," *Vehicular Technology, IEEE Transactions on,* vol. 43, pp. 439-446, 1994.

[11]   D. De La Vega*, et al.*, "Generalization of the Lee method for the analysis of the signal variability," *Vehicular Technology, IEEE Transactions on,* vol. 58, pp. 506-516, 2009.

[12]   B. Ai*, et al.*, "Novel statistical criteria for local mean power estimation in wireless coverage prediction," *Microwaves, Antennas & Propagation, IET,* vol. 5, pp. 596-604, 2011.

[13]   C. Tepedelenlioğlu*, et al.*, "Median filtering for power estimation in mobile communication systems," in *Wireless Communications, 2001.(SPAWC'01). 2001 IEEE Third Workshop on Signal Processing Advances in*, 2001, pp. 229-231.

[14]   D. Wong and D. C. Cox, "Estimating local mean signal power level in a Rayleigh fading environment," *IEEE transactions on vehicular technology,* vol. 48, pp. 956-959, 1999.

[15]   Y.-C. Ko and M.-S. Alouini, "Estimation of the local mean power over Nakagami fading channels," in *Personal, Indoor and Mobile Radio Communications, 2001 12th IEEE International Symposium on*, 2001, pp. C-107-C-112 vol. 1.

[16]   T. Jiang*, et al.*, "Kalman filtering for power estimation in mobile communications," *Wireless Communications, IEEE Transactions on,* vol. 2, pp. 151-161, 2003.

[17]   G. Pappas and M. Zohdy, "Extended Kalman Filtering and Pathloss modeling for Shadow Power Parameter Estimation in Mobile Wireless Communications," *Int. J. Smart Sens. Intell. Syst,* vol. 7, pp. 898-924, 2014.

[18]   W. C. Lee, "Estimate of local average power of a mobile radio signal," *Vehicular Technology, IEEE Transactions on,* vol. 34, pp. 22-27, 1985.

[19]   S. Mockford*, et al.*, "Local mean signal variability in rural areas at 900 MHz," in *Vehicular Technology Conference, 1990 IEEE 40th*, 1990, pp. 610-615.

[20]   M. Das and A. Cooprider, "New techniques for detection of changes in the local mean of a signal," in *Circuits and Systems, 1997. Proceedings of the 40th Midwest Symposium on*, 1997, pp. 849-852.

[21]   D. Avidor and S. Mukherjee, "Estimation and prediction of the local mean signal power in mobile systems," in *Vehicular Technology Conference, 2001. VTC 2001 Spring. IEEE VTS 53rd*, 2001, pp. 2751-2755.

[22]   Y. L. De Jong and M. H. Herben, "Prediction of local mean power using 2-D ray-tracing-based propagation models," *Vehicular Technology, IEEE Transactions on,* vol. 50, pp. 325-331, 2001.

[23]   S. Wei and D. L. Goeckel, "Error statistics for average power measurements in wireless communication systems," *Communications, IEEE Transactions on,* vol. 50, pp. 1535-1546, 2002.

[24]   W. LIN*, et al.*, "Radio Small-scale Fading around High-speed Railway [J]," *China Railway Science,* vol. 3, p. 020, 2004.

[25]   T. Kurt*, et al.*, "Adaptive Kalman filtering for local mean power estimation in mobile communications," in *Vehicular Technology Conference, 2006. VTC-2006 Fall. 2006 IEEE 64th*, 2006, pp. 1-4.

[26]   G. Zhu*, et al.*, "Modifying Lee Method of Estimating Local Mean Signal Power," *Journal of Internet Technology,* vol. 11, pp. 123-127, 2010.

[27]   R. Jadhavar and T. Sontakke, "2.4 GHz Propagation Prediction Models for Indoor Wireless Communications Within Building"," *International Journal of Soft Computing and Engineering (IJSCE),* vol. 2, pp. 108-113, 2012.

[28]   E. Tanghe*, et al.*, "The industrial indoor channel: large-scale and temporal fading at 900, 2400, and 5200 MHz," *Wireless Communications, IEEE Transactions on,* vol. 7, pp. 2740-2751, 2008.